AD-A096 312 STANFORD UNIV CA INST FOR PLASMA RESEARCH F/G 3/2
NOTES FROM THE STANFORD SUN-WEATHER WORKSHOP, 11-15 AUGUST 1980--ETC(U)
DEC 80 C R CLAUER N00014-76-C-0207
UNCLASSIFIED SU-IPR-825 NL

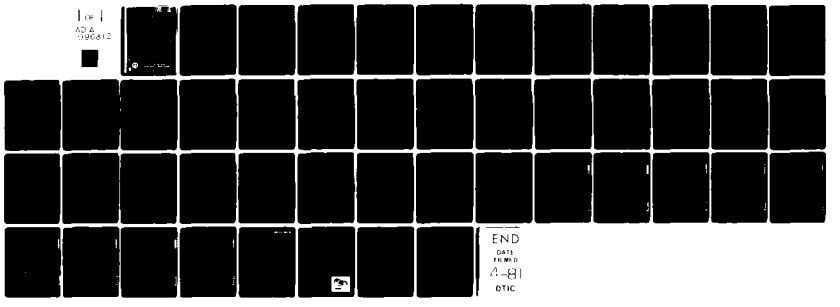

LEVEL II

NOTES FROM THE STANFORD SUN-WEATHER WORKSHOP

11-15 AUGUST 1980

by

C. Robert Clauer

Max C. Fleischmann Foundation
Grant T-8059-A

SUIPR Report No. 825

December 1980

INSTITUTE FOR PLASMA RESEARCH
STANFORD UNIVERSITY, STANFORD, CALIFORNIA

NOTES FROM THE STANFORD SUN-WEATHER WORKSHOP

11-15 AUGUST 1980

by

C. Robert Clauer

Max C. Fleischmann Foundation
Grant T-8059-A

A

SUIPR Report No. 825

December 1980

Institute for Plasma Research
Stanford University
Stanford, California

(14, SU-IPR...

SECURITY CLASSIFICATION OF THIS PAGE (When Data Entered)

REPORT DOCUMENTATION PAGE	READ INSTRUCTIONS BEFORE COMPLETING FORM
1. REPORT NUMBER: SUIPR Report No. 825	2. GOVT ACCESSION NO.: AD A096312
3. RECIPIENT'S CATALOG NUMBER	
4. TITLE (and Subtitle): Notes From The Stanford Sun-Weather Workshop, 11-15 August 1980.	5. TYPE OF REPORT & PERIOD COVERED: Scientific; Technical
6. PERFORMING ORG. REPORT NUMBER	
7. AUTHOR(s): C. Robert Clauer	8. CONTRACT OR GRANT NUMBER(s): T-8059-A; N0014-76-C-0207
9. PERFORMING ORGANIZATION NAME AND ADDRESS: Institute for Plasma Research, Stanford University, Stanford, California 94305	10. PROGRAM ELEMENT, PROJECT, TASK AREA & WORK UNIT NUMBERS
11. CONTROLLING OFFICE NAME AND ADDRESS: Office of Naval Research, Electronics Program Office, Arlington, Virginia 22217	12. REPORT DATE: December 1980 13. NUMBER OF PAGES: 32
14. MONITORING AGENCY NAME & ADDRESS (if different from Controlling Office)	15. SECURITY CLASS. (of this report) 15a. DECLASSIFICATION/DOWNGRADING SCHEDULE

16. DISTRIBUTION STATEMENT (of this Report)

This document has been approved for public release and sale; its distribution is unlimited.

17. DISTRIBUTION STATEMENT (of the abstract entered in Block 20, if different from Report)

18. SUPPLEMENTARY NOTES

Tech; Other

19. KEY WORDS (Continue on reverse side if necessary and identify by block number)

Sun-Weather
solar variability

20. ABSTRACT (Continue on reverse side if necessary and identify by block number)

A Workshop on solar variability and its relationship to weather and climate was convened at Stanford University on August 11-15, 1980. The purpose of the Workshop was to allow a free exchange of ideas between a group of solar physicists, geophysicists and Meteorologists interested in sun-weather relationships. These notes summarize much of the discussion at the Workshop.

DD FORM 1 JAN 73 1473 EDITION OF 1 NOV 65 IS OBSOLETE
S/N 0102-014-6601

UNCLASSIFIED
SECURITY CLASSIFICATION OF THIS PAGE (When Data Entered)

332630

Notes From The

Stanford Sun-Weather Workshop

11-15 August 1980

List of Participants

Dr. Robert Clauer
Dr. Robert Dickinson
Dr. W. Lawrence Gates
Dr. Bernhard Haurwitz
Dr. J. Murray Mitchell
Dr. Jerome Namias
Dr. Walter Roberts
Dr. Raymond Roble
Dr. Philip Scherrer
Dr. John Wilcox

List of Visitors

Dr. Jim Brasseur
Mr. Philip Duffy
Mr. John Foster
Mr. Todd Hoeksema
Dr. Joshua Knight
Dr. Chung Park
Dr. Peter Sturrock
Dr. Steve Suess

Preface

A Workshop on solar variability and its relationship to weather and climate was convened at Stanford University on August 11-15, 1980. The purpose of the workshop was to allow a free exchange of ideas between a group of solar physicists, geophysicists and meteorologists interested in sun-weather relationships. These notes summarize much of the discussion at the Workshop.

The notes are provided in outline form. They are intended to highlight important points which were made, action items, and to outline the general flow of the discussion. There are undoubtedly omissions. Nevertheless, the notes contain an excellent collection of ideas and I hope that they will help to maintain the excitement and momentum that were generated during the Workshop.

C. Robert Clauer

Stanford Sun-Weather Workshop

11-15 August 1980

I. List of Participants

Dr. Robert Clauer	Dr. J. Murray Mitchell	Dr. Philip Scherrer
Dr. Robert Dickinson	Dr. Jerome Namias	Dr. John Wilcox
Dr. W. Lawrence Gates	Dr. Walter Roberts	
Dr. Bernhard Haurwitz	Dr. Raymond Roble	

11 August 1980

I. Introductory Remarks

(Mitchell)

1. While there is no definitive proof of any sun-weather relationships, there are many suggestive studies.
2. Poorly done statistical studies unfortunately have added considerable confusion to the field.
3. It may be possible to begin to look beyond statistics now and examine physical mechanisms.
4. We know that the sun (solar wind) isn't dominant in control of the weather but solar variability (& solar wind variability) may contribute to weather variance
5. Will these studies be useful to weather prediction? -- probably not.
6. The research may, however, be useful to study mechanisms of weather variability. The observations may be useful as an exploratory diagnostic tool from which a physical understanding of physical connections may emerge.

II. Description of Solar Magnetic Fields

1. The large scale field is basically dipolar and reverses polarity every 11 years.
2. At lower latitudes the field structure is organized and can be described using the baseball seam analogy. These large scale features are stable on time scales of several years.
3. The seam maps into interplanetary space as a current sheet. During the last 11 years the interplanetary magnetic field was "away" from the sun above the current sheet and "toward" the sun below the sheet. The field near the baseball seam is closed. Away from the seam, however, the field is carried out from the sun by the plasma flow and is "open".
4. The baseball seam model is consistent with eclipse pictures of the corona
5. Coronal holes are generally found near the center of the "open" field line regions.
6. Coronal holes are sources of high speed streams.
7. Near the sun, magnetic fields dominate while beyond 2-3 solar radii, the plasma flow dominates the energy balance.
8. Solar wind plasma is highly conducting. This leads to the "frozen in flux" condition which causes the solar magnetic field to be carried outward into interplanetary space by the outward flowing solar plasma.

9. The 4 sector structure is fairly regular and is consistently observed in the photosphere. Observations of a 2-sector structure in the solar wind are probably the result of inadequate latitudinal sampling by spacecraft.

10. Evolution of the current sheet.
    a. At sunspot min. polar fields are the strongest, equatorial part is the weakest. There appears to be a decrease in the warp of the current sheet to be within $\pm 15^{o}$ of equator.

    b. At sunspot max. The opposite situation is observed. The warp of the current sheet can extend to as high as $\pm 50^{o}$ from the equator.

11. Sector boundary crossings are equivalent to current sheet crossings.
    a. The solar wind speed is typically a minimum near the boundary and a maximum about 3 days later.

    b. The magnitude of the interplanetary magnetic field B is typically a minimum near the boundary and a maximum near the middle of the sector.

    c. Observed cosmic ray flux is a maximum near the boundary and reaches a minimum 2-3 days later. This is understandable since V and B are a minimum near the boundary and therefore galactic cosmic rays have the easiest access. They will experience greater scattering near the center of a sector. These classical ideas on cosmic ray modulation are now being considerably revised.

III. Geomagnetic Response

1. Energy can be transferred from the solar wind to the magnetosphere. Certain conditions in the solar wind increase the efficiency of the energy transfer. The most important parameters appear to be the solar wind velocity V, the interplanetary magnetic field (IMF) magnitude B and the orientation of the IMF.

2. Two mechanisms have been proposed for the energy transfer.
    a. A "viscous" interaction between the solar wind flow and the geomagnetic field at the magnetopause boundary.

    b. Magnetic merging. Merging between the IMF and geomagnetic field can occur when components of the respective fields are antiparallel.

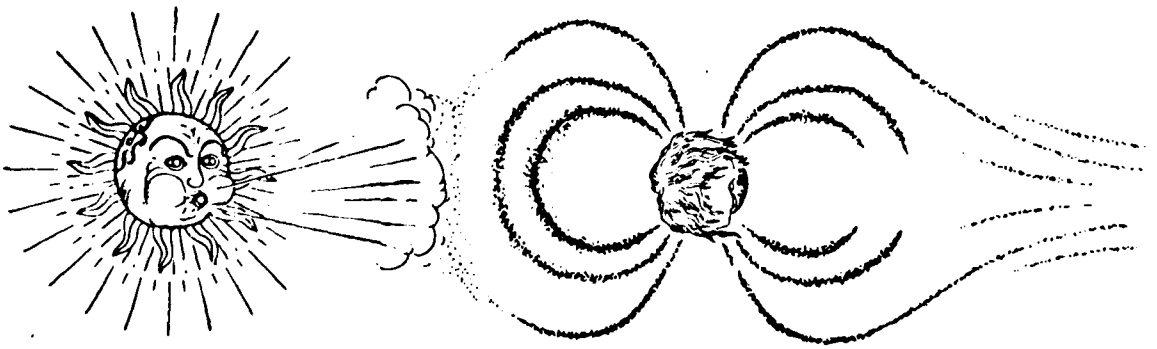

Fig. IV-11. A somewhat simplified view of the interaction between the solar wind and the Earth's magnetosphere (from the announcement of the advanced summer institute of reference 23-3).

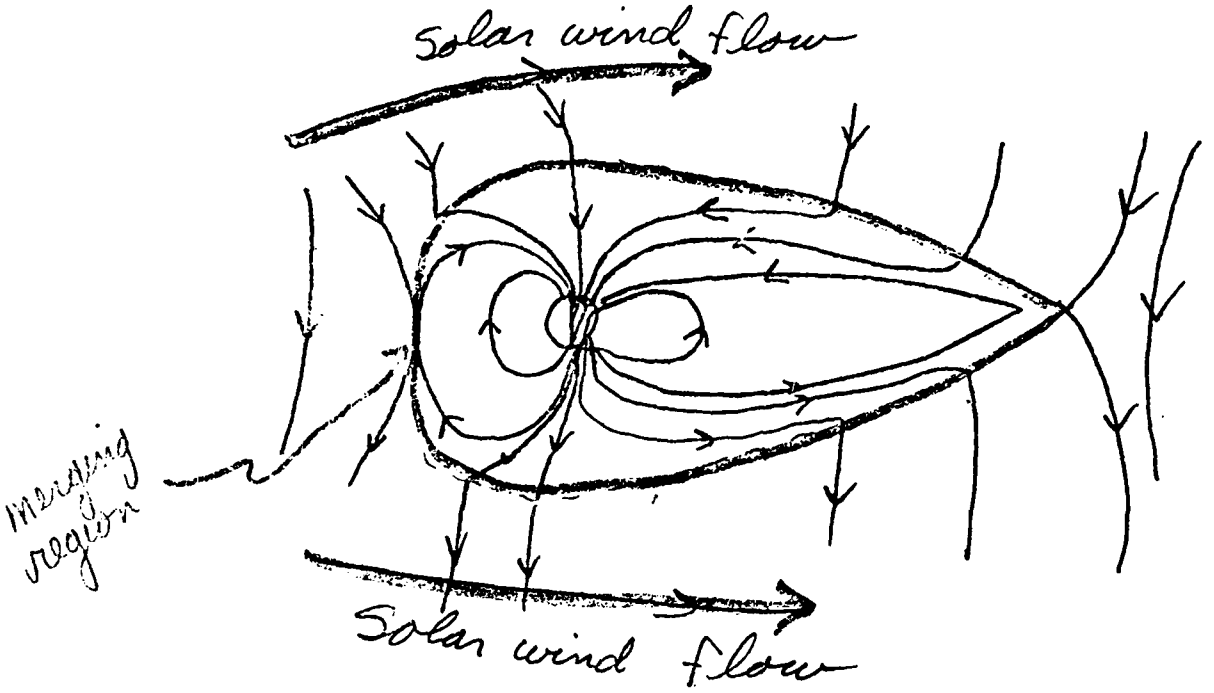

c. If one integrates the Maxwell Stress Tensor along the tail boundary, one can estimate the energy input to the magnetosphere.

3. How can this energy be deposited in the atmosphere?
   a. particle precipitation
   b. joule heating

Note by Roble: There is a data tape available which contains particle energy flux measurements recorded aboard a polar spacecraft. Derived parameters include the estimated energy input to the auroral zone by precipitating particles.

IV. The VAI Index

1. Roberts reported the history of the VAI development.

a. He originally examined the "persistence" of barometric pressure associated with a series of 27 day recurrent geomagnetic storms. There seemed to be a peak in the "persistence" 3-4 days after the peak in geomagnetic activity.

b. Another observation; strong low pressure centers off the Gulf of Alaska seemed deeper after periods of geomagnetic activity.

c. The VAI index was developed to take the subjectivity out of the above observation. It provided a quantitative objective parameter to replace his "trough index". The VAI was adjusted to select strong cyclonic systems.

d. The original studies only investigated the area around the Gulf of Alaska.

2. Remarks by Namias:
The development of the Gulf of Alaska low is very explosive. It appears to be dependent upon the local wind direction -- if it is from the north, the

explosive development proceeds. The development of the Gulf of Alaska low is a winter phenomenon. The effect is more striking when associated with a ridge having retrograde motion.

Suggestion: Is there a connection between the solar wind and abnormal wind shifts? Try a VAI & wind direction correlation. Should also examine the Kamchatka low which is associated with the Gulf of Alaska low. Also could study anomaly lists, maps of anomalies are easily attainable.

V. Examination of Individual Troughs

1. VAI of troughs is larger for away fields (Wilcox et al., 1979)

2. There is no known difference between away and toward fields which can presently explain this result.

3. This was done at 180^{o} longitude only.

4. Proposed individual trough study:
   a. use entire northern hemisphere.
   b. identify a trough anywhere when it develops.
   c. follow trough (every 12 hours).
   d. compute parameters for trough: VAI, lat, long, etc.
   e. perform study over entire year's data.
   f. Scherrer has automated this process.
   g. 15 years of 500mb data is available for this study.
   h. plan to see if results similar to Gulf of Alaska low can be obtained for Icelandic low. Namias notes that different mechanisms are responsible for the formation of the Icelandic Low. The differences were not discussed.

12 August 1980

I. Amplification of the discussion of cyclogenesis in the Gulf of Alaska by Namias.

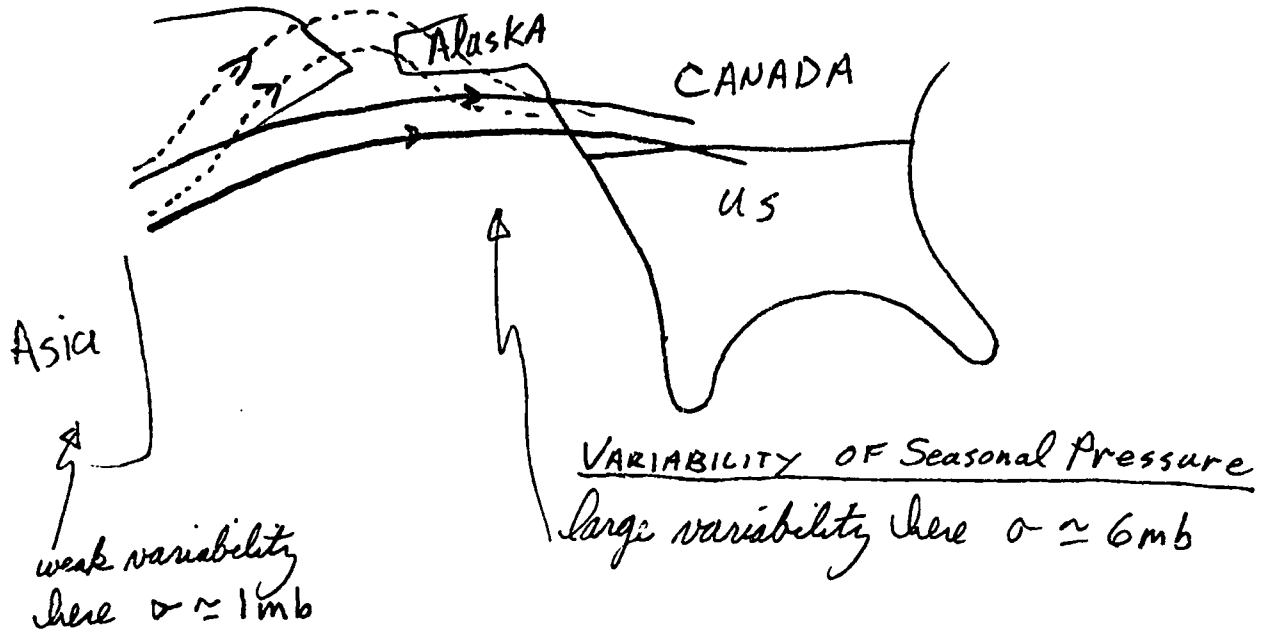

1. If the solid flow changes to the dashed flow a wind from the north of Alaska comes over the Gulf (cold air over warm water).
2. Convective activity begins rapidly
   air -40° from Alaska
   Water 0° in Gulf
   the large convection produces the low
3. The geography is also important - the low is produced in the lee of the mountains.
4. The low affects upstream dynamics. It appears to "push back" the ridge
5. Conclusion: A small perturbation can occur and non linear effects produce a large change.
6. Suggestions for analysis of 500 mb heights
   a. take "Away" average
   b. take "Toward" average
   c. examine individual winters
   d. use atlas to examine individual anomalies
7. Question: Is there a stable flow condition and an unstable flow condition which will respond to a small perturbation? Can these conditions be identified?
8. Suggestion: This may be manifest in terms of the number of Rossby wave nodes e.g. Tag data into 2 sets (away & toward) examine amplitude & phase behavior of long and short period waves.

9. Suggestion: Detailed case study of events which show greatest sun-weather effect.
   a. Compositing is an alternative to a case study.
      e.g. Cyclones in Away sectors
           Cyclones in Toward sectors

10. Note:during 1956-59 water in North Pacific was abnormally warm. This is interesting since the Roberts and Olson VAI sun-weather effect was strong during this period and diminished in early 60's. A possible related index to consider is thus the temperature of the North Pacific surface water.

II. Discussion of Vorticity by James Brasseur - See following pages.

VORTICITY, TOTAL CIRCULATION AND THE VAI

by

JAMES G. BRASSEUR *

(slides from discussion on 12 August, 1980)

* Present address:
Ames Research Center, NASA
Mail Stop 229-1
Moffett Field, CA 94035
(415) 965-6200

VORTICITY

$\vec{\omega} \Rightarrow$ spin of a fluid element

$$\vec{\omega} = \text{curl}\ \vec{v}$$

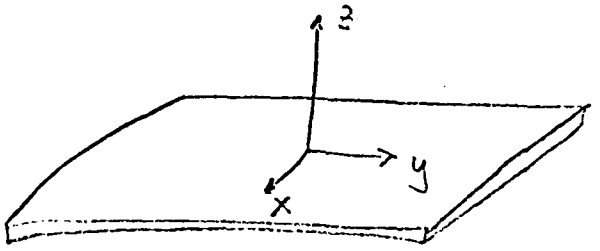

$$\omega_z = \frac{\partial v_y}{\partial x} - \frac{\partial v_x}{\partial y}$$

ABSOLUTE VORTICITY (INERTIAL FRAME)

$$\vec{\omega} = \text{curl}\ \vec{v} + 2\vec{\Omega}$$

$\vec{\Omega}$ ← angular velocity of rotating earth

$$\omega_z = \frac{\partial v_y}{\partial x} - \frac{\partial v_x}{\partial y} + f$$

$$f = 2\Omega \sin L$$

L ← latitude

LOW PRESSURE SYSTEMS

PEAKS IN ω_z ARE ASSOCIATED WITH TROUGHS IN PRESSURE (a low pressure system defines a vortex)

see contour plots

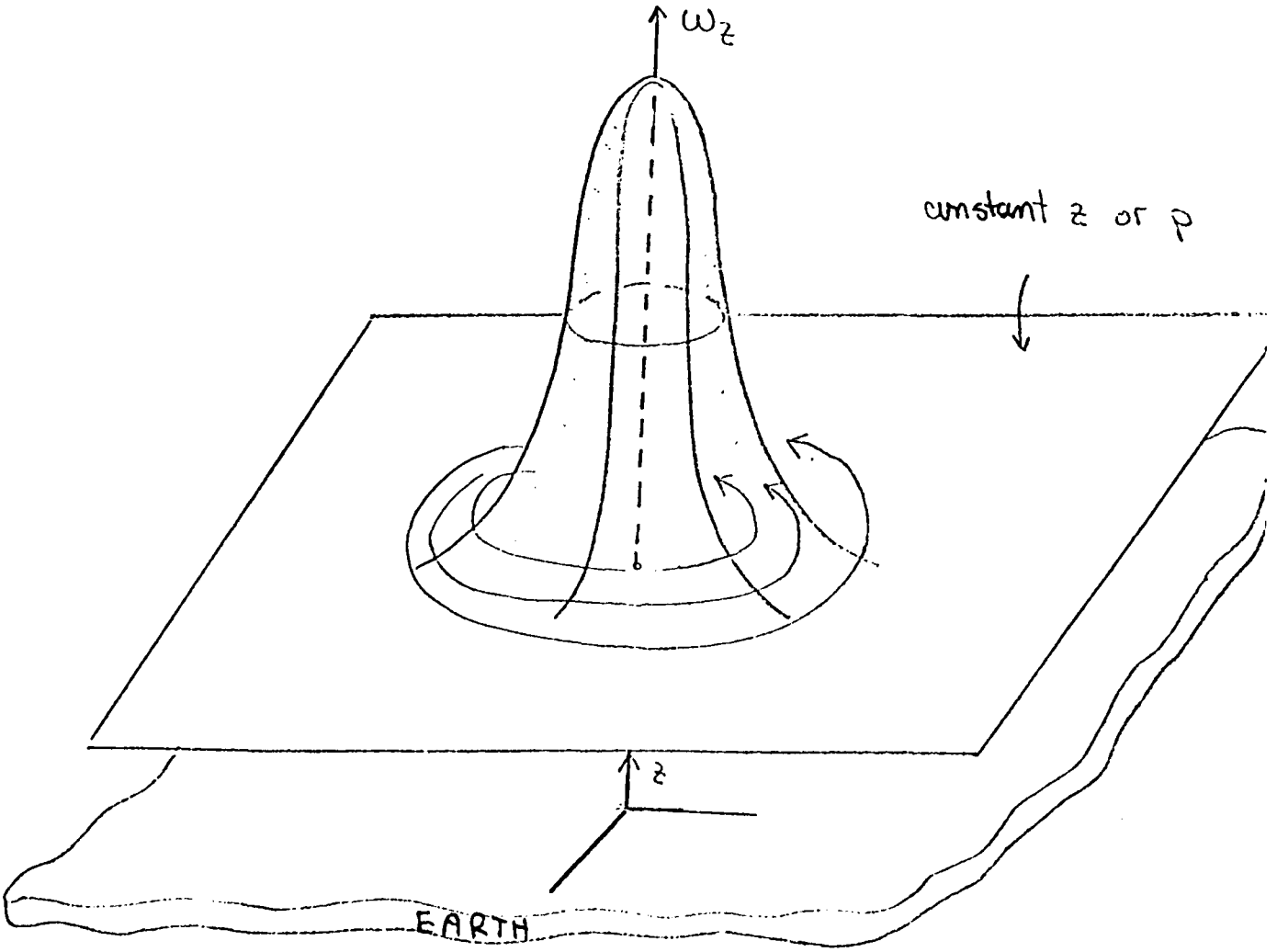

HEIGHTS

26 Feb, 1967 300mb Φ UT Inc: 60 m first: 8.00×10^3 m

red 7.9522 → 8.415
green 8.415 → 8.868 km
blue → 9.322
black → 9.7747

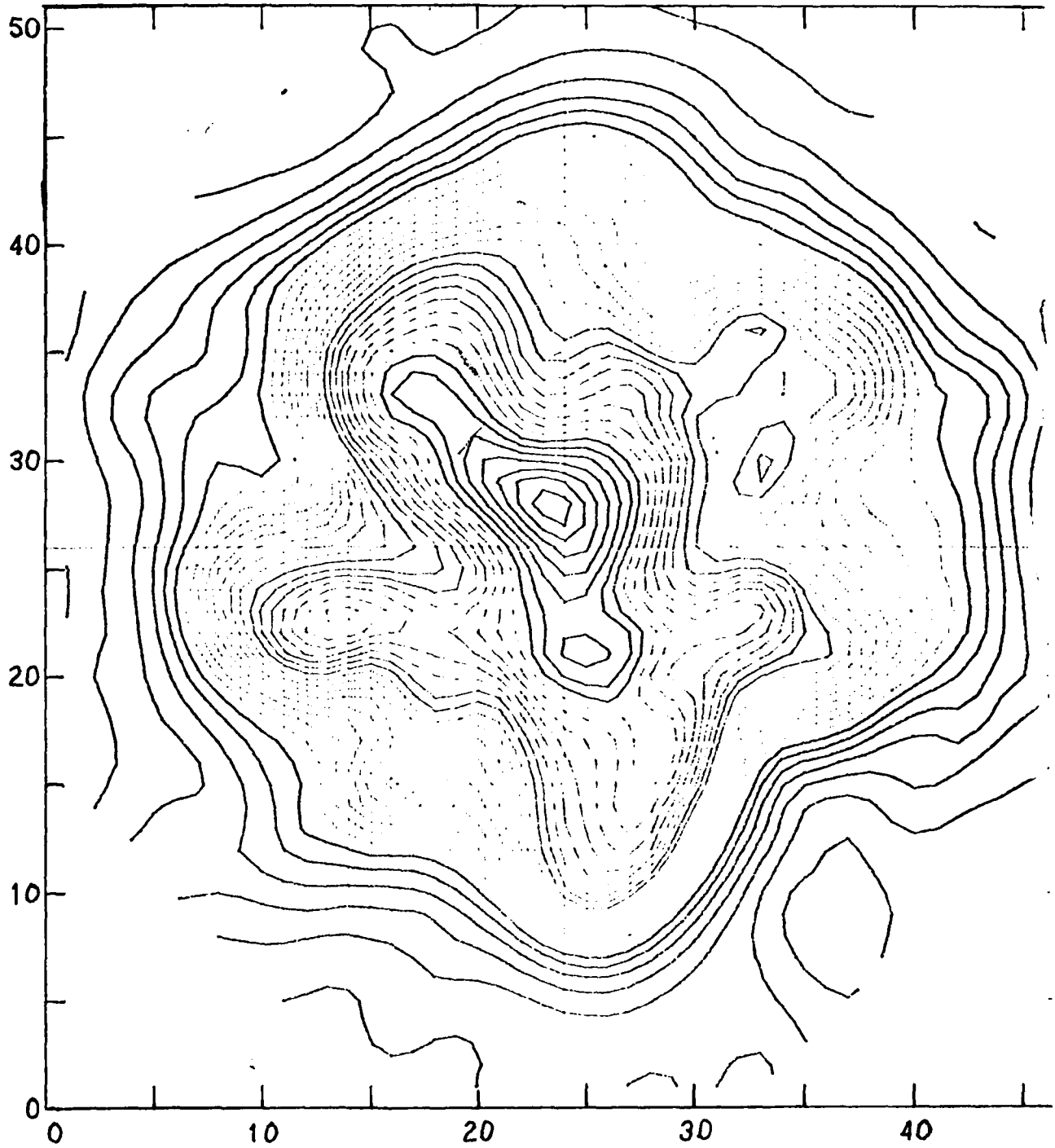

VORTICITY from Heights to OCSAT

26 Feb 1967 300mb ΦUT Inc: 2×10^{-5} sec^{-1} First : 0

min : -2.6

max: 37.9

(i) continuum or "background" vorticity shown in red from 0 up to and including 14×10^{-5}

(ii) green $16 \leq$ vorticity ≤ 20 (iii) black : vorticity ≥ 24

(iii) blue $20 \leq$ " < 24

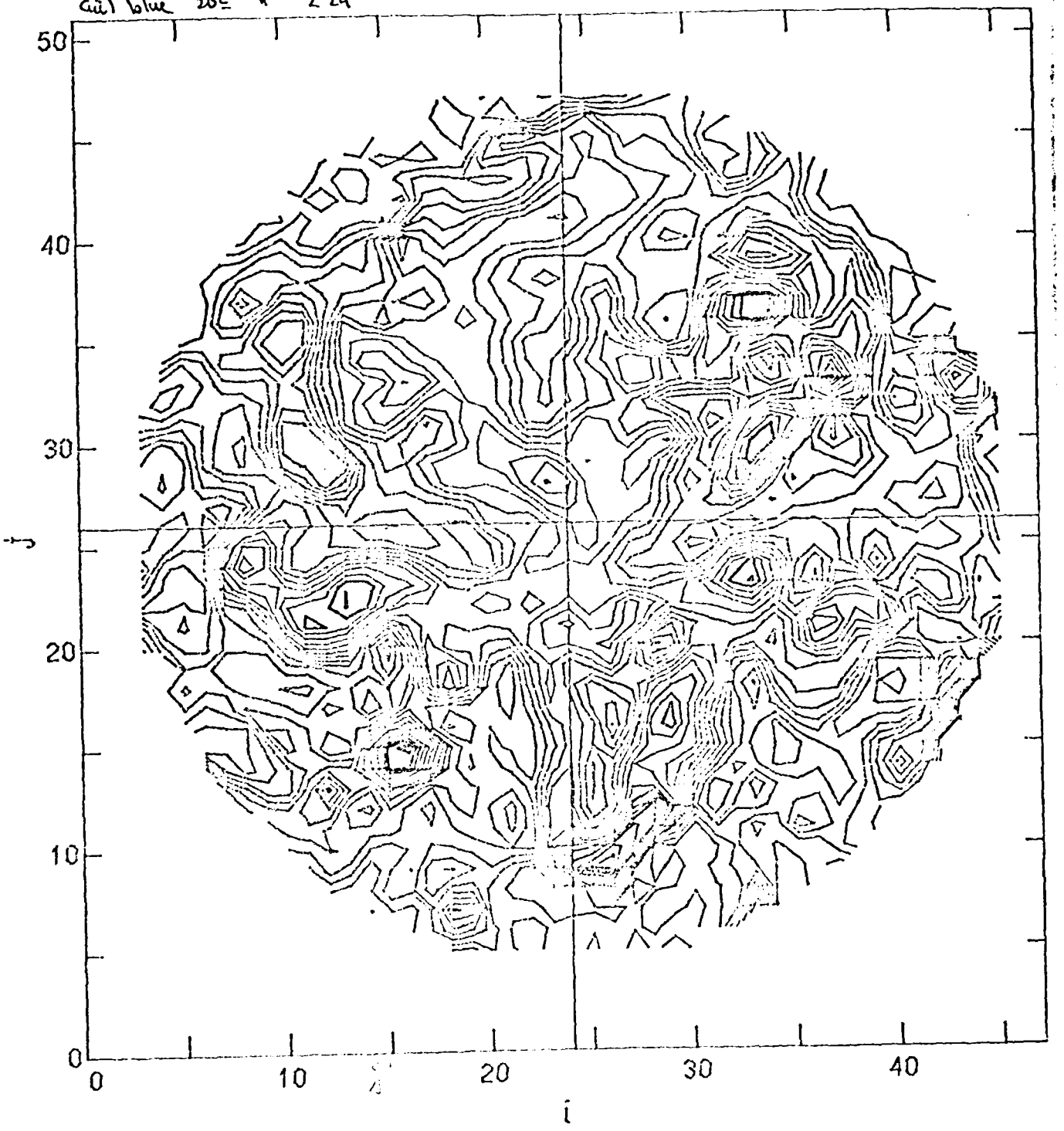

THE VAI

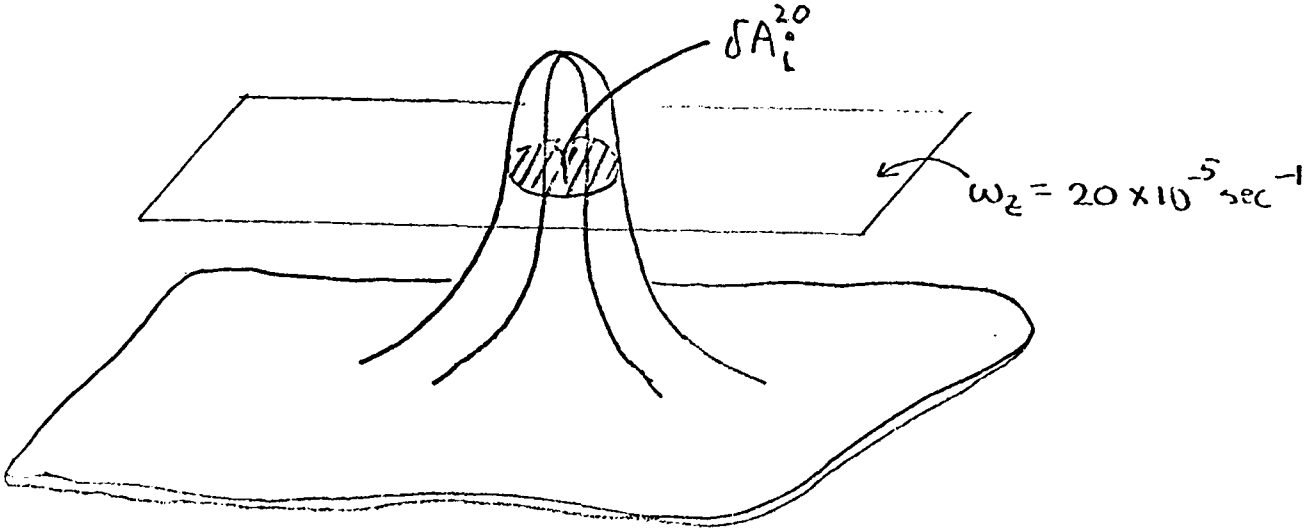

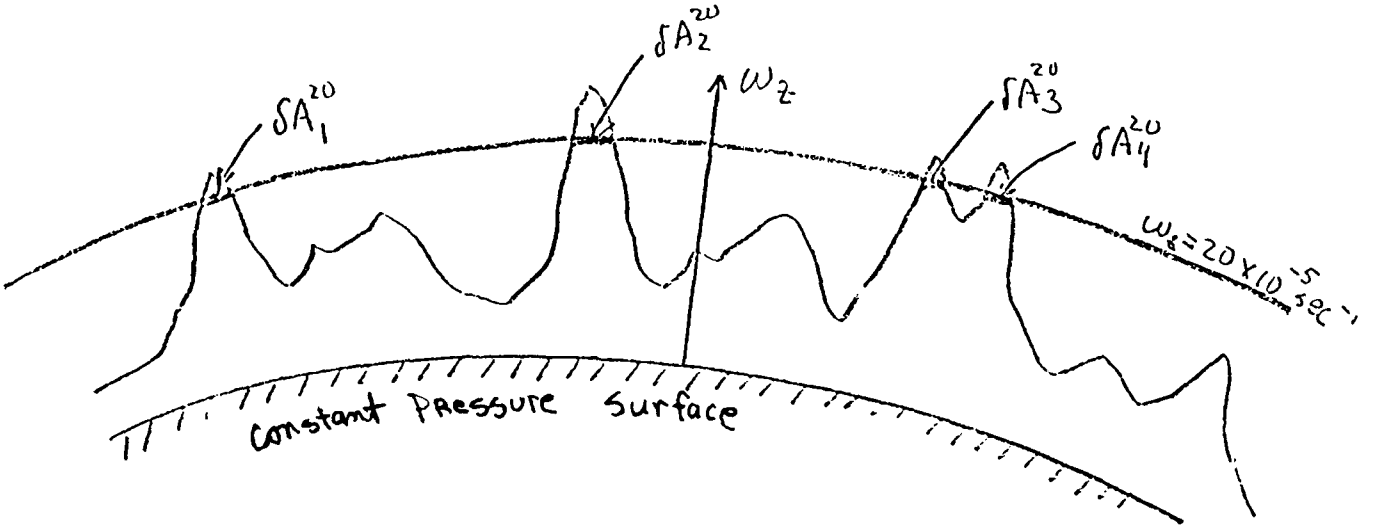

$$VAI = \sum \delta A_i^{20} + \sum \delta A_i^{24}$$

* see contour plots *

THE VAI

POINTS TO NOTE:

(1) The discriminator (eg, 20×10^{-5} sec^{-1}) can be thought of as a device to pick out low pressure systems which are particularly strong.

(2) The VAI is the sum of areas within closed contours and directly represents only a small fraction of the total area in the northern hemisphere.

(3) HOWEVER, in an indirect way the VAI actually represents an effect that is spread out over a much larger area (the "tip of an iceberg")

TOTAL CIRCULATION

Total circulation (or strength) of the vortex low pressure system is (inertial system):

$$\Gamma = \iint_A \omega_z \, dA$$

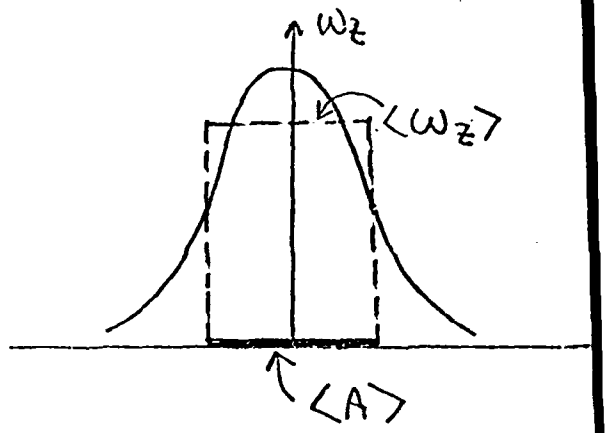

or

$$\Gamma = \langle \omega_z \rangle \langle A \rangle$$

↳ average vorticity ↳ average area

(eg, define $\langle A \rangle$ as area under the half maximum and $\langle \omega_z \rangle = \Gamma / \langle A \rangle$)

Thus a change in Γ might show up in

(i) change in $\langle \omega_z \rangle$

(ii) change in $\langle A \rangle$

DYNAMIC CHANGES IN Γ

* in the inertial frame:

$$\frac{D\Gamma}{Dt} = I_{viscous} + I_{BAROCLINIC}$$

$I_{viscous} \cong 0$ except at surface

$$I_{baroclinic} = \iint_A \vec{S} \cdot d\vec{A}$$

where $\vec{S} = \nabla P \times \nabla \frac{1}{\rho} = \nabla T \times \nabla s$

(perfect gas)

* examples: condensation (releases heat)
evaporation (absorbs heat)

* in the rotating frame

$$\left[\frac{D\Gamma}{Dt}\right]_{rotating} = \frac{D\Gamma}{Dt} - \frac{D(fA)}{Dt}$$

* NOTES (1) would like to analyse VAI in terms of Γ

(2) expect VAI to be related to $\langle A \rangle$

Γ and the VAI

$$\Gamma = \langle \omega_z \rangle \langle A \rangle$$

How would A CHANGE IN $\langle A \rangle$ RELATE TO A CHANGE IN VAI?

CASE I : Consider $\langle \omega_z \rangle$ constant

$\Rightarrow$ a decrease in VAI results from a decrease in $\langle A \rangle$

$\Rightarrow$ a decrease in Γ

(it is not clear how such a change would come about from sector perturbations)

(a more probable mechanism arises if we consider the following)

CASE II : Consider $\langle \omega_z \rangle$ changing and Γ constant

Then a reduction in VAI occurs in two ways (next figure)

(1) $\langle \omega_z \rangle$ decreases and $\langle A \rangle$ increases

(2) $\langle \omega_z \rangle$ increases and $\langle A \rangle$ decreases

* ie : VAI results from a REDISTRIBUTION of ω_z rather than a baroclinic change in Γ

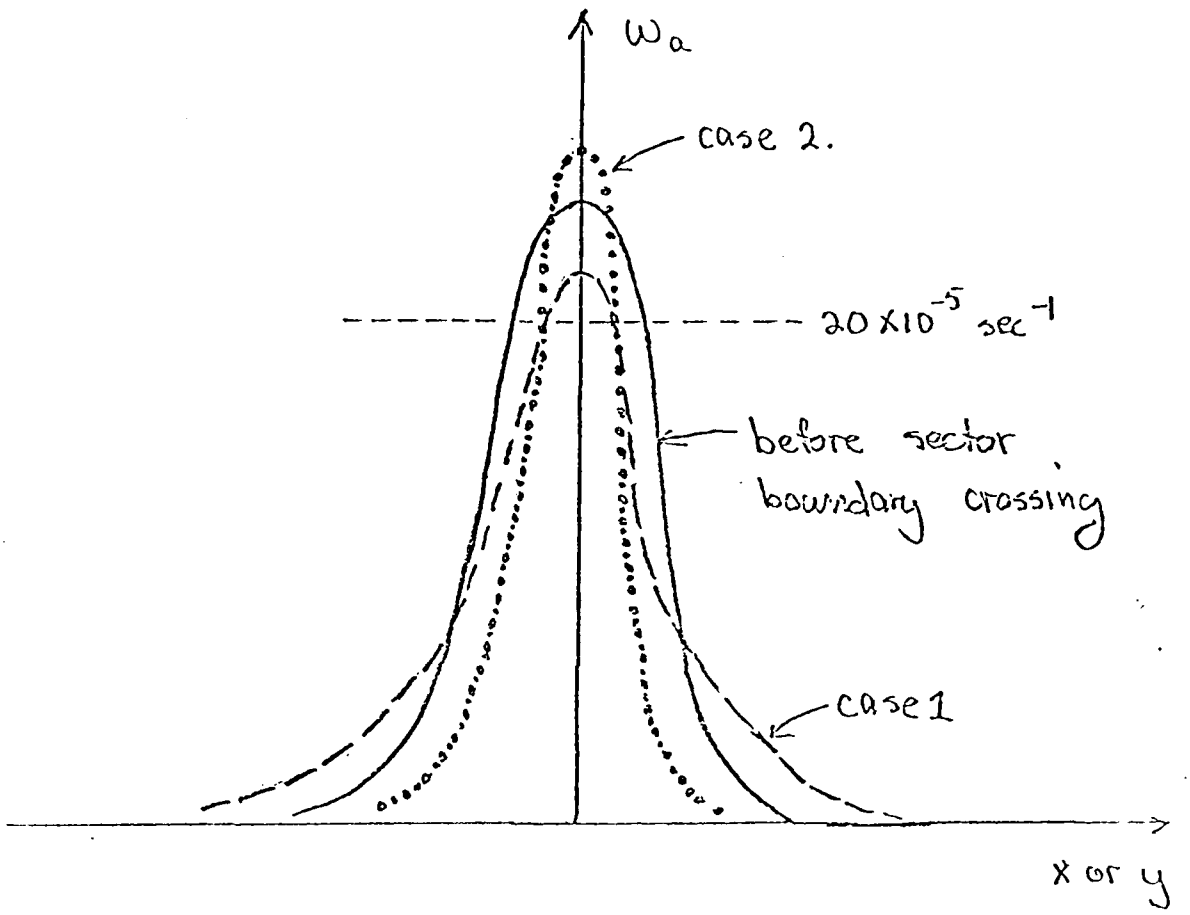
ω_a
case 2.
20×10^{-5} sec^{-1}
before sector boundary crossing
case 1
x or y

FIGURE 4

VORTEX STRETCHING

A Redistribution of $\omega_z \Rightarrow$
VERTICAL WIND GRADIENTS
through the mechanism of vortex stretching.

eg, for Γ constant

$$\frac{D\omega_z}{Dt} \cong \frac{\omega_z}{\rho} \frac{\partial}{\partial z}(\rho w_z)$$

* (note: vortex stretching applies locally)

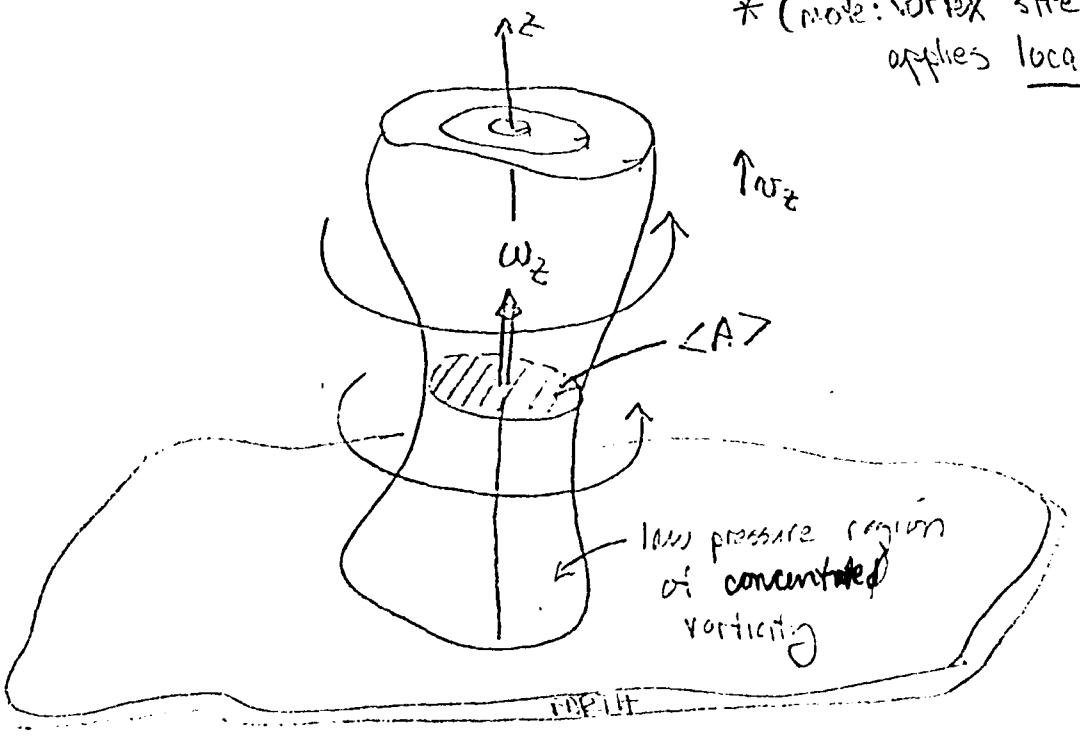

1. Conclusion: Brasseur proposes using a data set of total circulation computed for individual troughs. Then examine $\langle A \rangle \langle \omega \rangle$.

   Gates notes that data sets are presently available for such a study.

   Mitchell remarked that changes in the shape (pointiness) and position of a low wave number flow will produce a higher harmonic signal which really reflects a change in a low harmonic.

   Both Gates and Mitchell suggest that the sun-weather effect is most likely a low wave-number phenomenon.

III. Review New Stanford Sun-Weather Data Set

1. Plan to use the data set in the manner described yesterday in order to compare with past work.

2. Concurrently, would like to develop more physically meaningful parameters and search for causal links.

3. Roberts reviewed again what was done in the '50's.
   a. The analysis revealed a geomagnetic activity (driven by the solar wind)-weather effect.

   b. The effect: low pressure centers seemed deeper after periods of geomagnetic activity.

   c. The effect focused on troughs that first appeared east of 180° on 3rd day after the peak of a large geomagnetic disturbance.

   d. The effect was observed to be strongest using his original trough (depth/width and contour length) indices - the effect was somewhat weaker in the VAI index.

   e. This was a fortuitous choice of time period since the effect appeared strongest in the data from 1956-59.

4. Scherrer gave a brief description of the NCAR mini computer and graphics system.
   a. Goal is to expedite the process of identifying the evolution of individual troughs or vorticity centers so that a large amount of data can be utilized (15 years of bi-daily observations).

   b. It is fairly easy to identify the trough, more difficult to identify associated centers.

   c. A method to deal with this problem is to identify a trough and add vorticity centers within the trough -- further discussion on the details of this problem was deferred.

   Note: The Historical Map Series 500mb troughs were tracked for several days. This series was compiled for the period (1895-present) and may contain a catalogue of active centers.

IV. Discussion of the Hemispheric VAI Result

1. Described in the paper Wilcox et al., 1976. Fig. 1 shows the original result.

2. MEV proton streams which are associated with some sector boundaries select an interesting subset of events, Wilcox, 1979b

3. The proton stream lasts about 3 days.

4. The protons are accelerated by shocks formed by high speed streams catching up with slower plasma flow. The region where a high speed stream interacts with the slower plasma has been called an interaction region. Interaction regions are associated with high geomagnetic activity because of the large B fields, particularly the fact that large southward IMF is generally developed in the interaction region.

5. Remarks (preprint Wilcox and Scherrer, 1980.)
   a. A careful examination of latitude and height effects should probably be performed again, particularly with the goal of identifying propagation effects.

   b. Dickinson suggests the Vorticity Strength Index

      $=\int (W-16\cdot 10^5)dA$

      to replace VAI. (from Fig. 2)

   c. No clear understanding of the discontinuities in Fig. 4. No documented change in analysis procedures.

   d. Roberts recalls a change in the character of Auroral activity around 1962 reported by the SEL forecast center -- he will investigate.

13 August 1980

I. Initial Remarks

1. We note that most results which suggest a sun-weather effect show a fast response (sometimes less than a day) and a long persistence (sometimes as much as 14 days).
2. Gates: Have you examined sea level pressure for the sun-weather effect?
   Answer: Rostoker has examined sea level VAI and sector boundaries, the results were partially consistent with Wilcox's work.
   a. Advantage of sea level data is the large amount of it.
   b. The sun-weather effect using VAI appears to maximize at 300-500 mb and decreases markedly above the tropopause.
3. Discussion of the plot of zonal index for A and B days.
   a. Zonal index designed to describe general circulation
   b. Zonal index is average zonal winds between 35°-55° latitude.
   c. Indices are also created for the latitude bands 55°-70° and 35°-20°.
   d. The figure shows that there is a minimum in VAI about 4 days after a minimum in the zonal index.
   e. Namias agrees that the explosive development in the Gulf of Alaska would be more probable with a low zonal index. e.g. high index implies high winds and the geography forces the trough patterns which are fairly stable. With low index the trough patterns are more variable and thus the abnormally large Gulf of Alaska low is more likely.
   f. Suggestion: Plot zonal index I(t). Pick minima in I(t) as key times and examine VAI. Pick minima in VAI which are not related to sector boundaries and examine I(t).
   g. To use the compositing technique successfully (superposed Epoch maps) the maps must be normalized to remove the seasonal variability. Could do this using a 2 month running mean map.

II. Ohio State Review (Wilcox, 1979a)

1. Figure 3 of paper discusses result of Larsen & Kelly's figure 3 of forecast accuracy. (Larsen and Kelley, 1977).
   a. This is an analysis of forecast accuracy in a time frame related to sector boundary crossings.
   b. The result strongly suggests that a change in tropospheric circulation is occurring in association with the sector boundary crossing.
   c. While a sun-weather influence is indicated the result does not indicate if there is a consistent error in the forecast associated with sector boundaries.
   d. Should repeat the study of Larsen & Kelley. Look for consistent errors in the forecast, use fine mesh grid and hemisphere data, use homogeneous data set, study regional effects, use long term forecasts (e.g. 5 days), examine short term vs long term forecast accuracy.

III. Atmospheric Electricity (Roble)

1. Kinds of Effects

a. Solar flare effect

i) daily ground potential and earth current increased following a solar flare. Maximum occurs 3 days after flare.

ii) large ion production increase and electric field decrease has been observed by a stratospheric balloon following the August 1972 PCA event.

iii) Air-Earth current increases about 70% following a flare measured by balloons at South Pole.

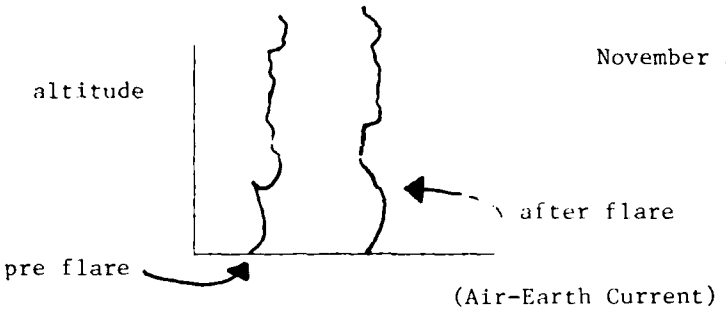

b. Sector boundary crossing effects

i) Air-earth current and E change following a sector boundary. The effect is different for + to - and - to + crossings (Fig 7 of Wilcox's Ohio State Rev., which show Reiter's observations) (Wilcox 1979a)

ii) Decrease in E following sector boundaries observed by Chung Park is opposite to the observation by Reiter.

c. Variations in air-earth current associated with geomagnetic activity. The variations have not been consistent, however, ordering the observations properly with respect to the dawn-dusk magnetospheric potential field may organize the observations.

d. There are changes in the diurnal variation of the ground electric field in the arctic as compared with low latitudes. These effects may be associated with changes in the magnetospheric electrical potential, but this coupling needs further study.

e. Air earth currents show a long term variation with the solar cycle having a larger current during solar minimum and smaller at solar maximum.

IV. Markson Paper (Markson and Muir, 1980)

1. Shows that the ionospheric potential $\propto \frac{1}{V_{sw}}$ and cosmic ray flux $\propto \frac{1}{V_{sw}}$ where V_{sw} = solar wind velocity, concludes that ionospheric potential is controlled by solar wind modulation of cosmic ray flux.

2. Plots of ionospheric potential vs Vsw passed out.
3. With atmospheric electricity, there is no clear coupling with the neutral atmosphere.
   a. Can it cause greater droplet coalescence efficiency in clouds?
4. If one had a mechanism to facilitate the development of thunderstorms, it could affect synoptic systems (Namias).
5. Comments
   a. Mitchell outlined alternative impacts of fair weather field on cumulonimbus cloud properties (relative validity needs checking):
      i) changes electrical activity of clouds that will become thunderstorms in in any case.
      ii) changes proportion of all cumulus clouds that become electrically active (i.e. thunderstorms).
      iii) changes total population of cumulus clouds (unlikely).
   b. An examination of satellite observations of visible and IR clouds associated with areas of VAI enhancement or minima may give a clue to whether cloud development is associated with the effect.
   c. Changes in the fairweather field would be expected to affect the dynamics of cumulonimbus clouds (not known if the effects are significant).
      i) Droplet collection efficiency would increase with E enhancement (result of numerical simulations).
      ii) E must affect the charge separation in the cloud initially, but then the large internal fields generated by the storm dominate and the fair weather fields are negligible by comparison.
   d. What are prethunderstorm fields in cumulonimbus clouds relative to fairweather field? This will determine how much effect one might expect to be due to the fairweather field.
   e. Data on Schumann Resonances may provide a data base which could relate thunderstorm activity to VAI. Most of the work on Schumann Resonances was done by Polk.
   f. The large scale environment is important to the problem which we are addressing. Can we get a mechanism which generates clusters of storms?
   g. Markson proposes a <u>geoelectric index</u> of the earth-ionosphere potential difference. What is the reaction to this proposal?
      i) The measurement is fundamental and important.
      ii) General opinion is that it is a worthwhile goal and should probably be supported.
      iii) A letter will be drafted and distributed regarding the usefulness of this measurement.

Stanford Sun-Weather Workshop

14 August 1980

I. Review the efficiency of forecasts

1. If forecast efficiency decreases are tied to a solar structure, this is compelling evidence for a sun-weather effect.
2. If the forecast efficiency decrease is "sizable" then the solar effect is "sizable".
3. Therefore, this is important and must be studied carefully.
4. The test must go beyond the 12 and 24 hour forecasts to use several-day forecasts.
5. Must look at both the conventional grid and fine mesh grid (the conventional grid is compatible with global analysis).
6. In addition to forcast statistics using VAI, probably should also examine more conventional parameters.
7. Since this is so important - may want to enlist the advice of a statistician to determine the significance of the result.
8. Suppose we do the forecast efficiency of VAI - so what does it mean? What is the physical mechanism that is being reflected in VAI? Perhaps should correlate VAI with other measures of circulation and weather.
9. Total circulation above some referance level could be a physically useful parameter.
10. Use an index of baroclinic structure and kinetic energy and see if these reflect changes in VAI.
11. Should we keep track of shear and curvature separately? Yes, this could separate out some mechanisms for producing vorticity.
12. Relative ridge-trough circulation may reflect something (some earlier work suggested no ridge effect related to solar sectors).
13. Method for test
    a. Hypothesis: something external is influencing the system e.g. sector boundaries.
    b. Use best numerical forecast; compute the error in the height field.
    c. Do this for many forecasts and determine the mean error.
    d. Compare the mean error with the anomalies e.g. sector passages.

    The best approach to isolating these things is to simulate the behavior as best as you can - look for deviations and then look for external stimulus of deviations.
14. (Haurwitz) Do you feel that forecasts are so good that this is a reasonable test? Ans: Indeed there are many errors. However, if the effect is in a systematic sense, the effect can be identified.

15. (Namias) There are step wise multiple regression techniques which relate the measurement at point A to all other global measurements which account for much of the variance.

16. (Roberts) Should probably make a large effort to find another more conventional parameter in the forecast which also contains the same effect as VAI.

17. (Mitchell) Devil's advocate view of VAI effect: Suppose that in the analysis of VAI data, the VAI value is high only when based on a nearby rawind report to confirm it. If during high geomagnetic activity rawind data is less available because of communication disruption, the VAI effect follows. Might be worth checking into.

18. Has there been any change in the frequency of Aurora seen at lower latitudes? Roberts has a qualitative feeling that they were more frequent in the 50's.

II. 22 Year Solar Cycle Variability

1. Solar field polarity changes on a 22 year cycle (the solar polar fields change polarity every 11 years).

2. Question- Most of the "spottedness" was in the N hemisphere during the last cycle - does that mean that most of the activity centers were in the North also? Answer, yes.

3. Location of sunspots migrates from mid latitudes to the equator during the 11 solar cycle,

4. The 11 year cycle is an average - it varies from 7-15 years.

5. There is a small but well defined 22 year wave in geomagnetic activity (Figures passed out).

Five steps are listed in the agenda to explain the 22 year variation in geomagnetic activity.

a. Solar magnetic polarity changes every 11 years. Therefore, the field above the current sheet will be "toward" for 11 years and "away" for 11 years (the opposite field is below the current sheet).

b. Solar field antiparallel to the geomagnetic field is most efficient for coupling solar wind energy to the magnetosphere.

c. There is an annual variation in the predominant polarity of the IMF observed in the vicinity of the earth because the earth's orbit is inclined to the solar equator.

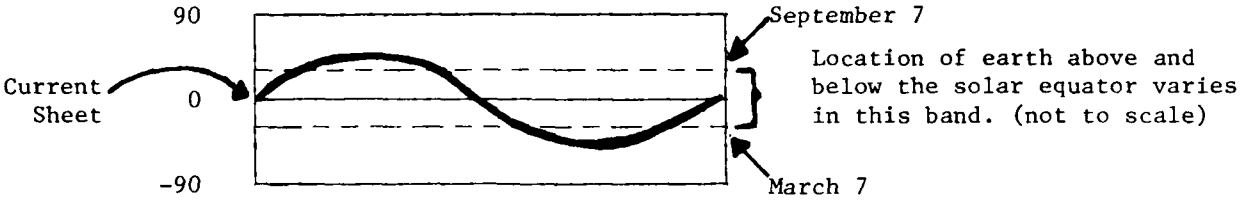

On December 7 the earth is at the solar equator
On March 7, 7° below equator
On June 7 at equator
On September 7, 7° above equator

Therefore, during half of the year "away" is predominant and half of the year "toward" is predominant.

The effect is greatest at sunspot minimum when the warp in the current sheet is the smallest, however it is clearly observable at sunspot maximum also.

d. At the equinoxes the tilt of the dipole and the spiral field combine to yield parallel or antiparallel field. The figures may be helpful to visualize this.

e. Combine the steps.

f. Could it be possible to add a few more steps and understand the 22-year cycle of droughts?

6. Note that we are in the rising part of the old cycle.

III. 22 Year Drought Cycle in Western U.S. (Mitchell et al., 1979)

1. Large area droughts tend to be favored near the beginning of odd solar cycles.

2. Maximum-area droughts tend to occur in maximum-amplitude sunspot cycles, minimum-area droughts during minimum-amplitude sunspot cycles.

3. The period of greatest drought risk follows the period of greatest recurrent-type geomagnetic activity by 2-3 years.

4. One suggestion, should geographically segregate data, e.g. Western droughts are different than plains droughts.

   Better to examine the area between the Continental Divide and Mississippi River.

5. A suggestion has been made that if you consider the 18.6 year lunar tidal cycle beating with the 22 year solar cycle - the drought data in the harmonic dial analysis becomes better organized - lying within one quadrant.

IV. Suggestions

1. Divide the list of sector boundary times into categories based on different "states" of circulation which may or may not be responsive to the sun-weather effect.

2. Still must consider other solar changes. The magnetic explanation should not be the only consideration.

3. What are the scale of magnetic activity changes and electric field changes which occur at sector boundaries and over the 22 year cycle?

Stanford Sun-Weather Workshop

15 August 1980

I. Conclusions, Remarks, Ideas

1. Heat flow measurements are available on the NMC grid. Could some analysis of this be useful?
(Dickinson) Would expect that an index similar to VAI would be required to pull out the temperature information. Circulation and thermal height fields are correlated.

2. The differential relation of the fields is important to generate vorticity.

3. Is there an observable change in heating associated with the sector boundary? This would be difficult to determine.

4. The surface pressure ought to be tested--especially over the oceans. Also surface pressure provides a long record of data (to 1899). Features in surface pressure may, however, be somewhat subtle.

5. Sector boundaries can be inferred back to 1926.

6. Hines idea: The VAI effect works by changing the phasing of the trough migration.

   Roberts showed example where the ridge movement in Alaska region affected the trough.

7. Should look at a numerical simulation for the example to see if it anticipates the ridge movement.

8. Teleconnection: Intra and Inter Regional Correlations.

   Correlate one grid point with all other grid points (e.g. for 700 mb height) and obtain a correlation field.

9. It would be interesting to get correlation maps (movie) as a function of time lag.

10. Using 5 day means, monthly means, and seasonal means produce very similar teleconnection patterns.

11. Flares are quite variable in terms of UV, X-ray, mass flux, etc.

12. Standardized anomoly maps could be used to organize VAI into categories.

13. Is it possible to create an index of stability (or susceptability to change)?

    There are patterns which are dynamically unstable.

    A more effective instability is baroclinic instability. In the mean it is stable but it can be locally unstable. An index of the average would show very little variation.

14. Idea by Mitchell: There are circulation progressions from season to season. If a

change does not occur at first, the system is increasingly stressed until the change occurs. This suggests that certain intervals of the seasons may be more appropriate to study. Select these stressed periods for study.

What are these critical periods?

What are the critical changes?

15. Larry Gates' Chain of Events
(see "Hypothetical Sequence in Sun-Weather Relationships" attached)

The suggestion is to make a controlled run and a test run with an altered parameter using the numerical weather models. Investigate the statistics of the two runs and search for VAI changes among other effects.

16. Should consider the possible solar influence on ionospheric potential.

17. How frequently does Bremsstrahlung penetrate and how low? Frequently observed at 30 km probably goes to 20 km. May get ion clusters at 15 km The cloud heights are roughly at 12 km. Therefore the modulation of CR could also play a role.

18. Should study timing relationships and the time sequence of events. Do changes begin in the auroral zone? Does the building of the ridge precede the development of the Gulf of Alaska low.

19. Is the ionospheric potential governed by the resistivity of the lower 5 km or by the resistivity of the few KM above the cumulonimbus?

20. The Svalgaard (1973) paper has an important and interesting result which should be confirmed. (This paper mailed out to everyone).

Polar height up; lower latitude height down after sector passage. This will decrease the zonal circulation.

II. Summary Comments, Thank yous, Goodbyes, etc.

Acknowledgements

Support for the Stanford Sun-Weather Workshop was provided by a grant from the Max C. Fleischmann Foundation.

A Hypothetical Sequence in Sun-Weather Relationships

sector boundary passage, ...

↓

change in cosmic ray flux, ...

↓

change in ionospheric potential / magnetic field

must likely modulate to penetrate to troposphere fairly enough.

↓

change in atmos. electric field
(~ 10-20%, global ?)

auroral → Bremstrahlung → ion clusters → nucleation

↓

change in penetrating convection
(especially over oceans in mature lows in winter)

↓

change in net latent heating in upper troposphere

↓

change in upper tropospheric temperature field

↓

change in baroclinity, eddy kinetic energy, ...

↓

change in vorticity, VAI, ...

atmos. model

REFERENCES

Hays, P.B., Roble, R.G., A quasi-static model of global atmospheric electricity 1. The lower atmosphere, J. Geophys. Res., 84, 3291, 1979.

Larsen, M.F., and Kelley, M.C., A study of an observed and forecasted meteorological index and its relation to the interplanetary magnetic field, Geophys. Res. Lett. 4, 337, 1977.

Markson, R., and Muir, M., Solar wind control of the earth's electric field, Science, 208, 979, 1980.

Mitchell, J.M., Stockton, C.W., and Meko, D.M., Evidence of a 22-year rhythm of drought in the western United States related to the hale solar cycle since the 17th century, B.M. McCormac and T.A. Seliga (Eds.): Solar-Terrestrial Influences on Weather and Climate. 125-143, by D. Reidel Publishing Company, Dordrecht, Holland, 1979.

Roble, R.G., and Hays, P.B., A quasi-static model of global atmospheric electricity 2. Electrical coupling between the upper and lower atmosphere, J. Geophys. Res., 84, 7247, 1979.

Schatten, K.H., Statistical proof vs. statistical motivation, EOS, 61, 506, 1980.

Svalgaard, L., Solar activity and the weather, D.E. Page (Ed.) Correlated Interplanetary and Magnetospheric Observations, 627-639, by D. Reidel Publishing Company, Dordrecht-Holland, 1974.

Wilcox, J.M., Influence of the solar magnetic field on tropospheric circulation, B.M. McCormac and T.A. Seliga (Eds.): Solar-Terrestrial Influences on Weather and Climate. 149-159, by D. Reidel Publishing Company, Dordrecht, Holland, 1979a.

Wilcox, J.M., Tropospheric circulation and interplanetary magnetic sector boundaries followed by MeV proton streams, Nature, 278, 840, 1979b.

Wilcox, J.M., Duffy, P.B., Schatten, K.H., Svalgaard, L., Scherrer, P.H., Roberts, W.O., and Olson, R.H., Interplanetary magnetic field polarity and the size of low-pressure troughs near 180° W longitude, Science, 204, 60, 1979.

Wilcox, J.M., Hoeksema, and Scherrer, P.H., Origin of the warped heliospheric current sheet, Science, 209, 603, 1980.

Wilcox, J.M., Scherrer, P.H., On the nature of the apparent response of the vorticity area index to the solar magnetic field, Solar Physics, 1980

Wilcox, J.M., Svalgaard, L., and Scherrer, P.H., On the reality of a sun-weather effect, J. Atmos. Sci., 33, 1113, 1976.

Wilcox, J.M., Scherrer, P.H., Svalgaard, L., Roberts, W.O., Olson, R.H. and Jenne, R.L., Influence of solar magnetic sector structure on terrestrial atmospheric vorticity, J. Atmos. Sci., 31, 581, 1974.

THE ASTROPHYSICAL JOURNAL, 241:811–819, 1980 October 15

THE ROTATION OF THE SUN: OBSERVATIONS AT STANFORD

PHILIP H. SCHERRER, JOHN M. WILCOX, AND LEIF SVALGAARD[1]

Institute for Plasma Research, Stanford University

Received 1980 February 11; accepted 1980 April 11

ABSTRACT

Daily observations of the photospheric rotation rate using the Doppler effect have been made at the Stanford Solar Observatory since 1976 May. These observations show no daily or long-period variations in the rotation rate that exceed the observational error of about 1%. The average rotation rate is the same as that of the sunspots and the large-scale magnetic field structures.

Subject headings: Sun: rotation

I. INTRODUCTION

Measurements of the photospheric rotation rate using the Doppler effect have been the subject of controversy ever since they were first made (e.g., Plaskett 1915; DeLury 1939; Hart 1954; Howard and Harvey 1970; and Plaskett 1973) and have been recently reviewed by Howard (1978). Daily observations at the Stanford Solar Observatory (SSO) have been made since 1976 May. Analysis of the 731 full-disk low-resolution Dopplergrams made to date yields results that conflict with some other recent sets of observations. The SSO observations show no daily or long-period variations in the rotation rate that exceed observational error, and the average rate is about the same as that of the large-scale magnetic field structures and sunspots. These conclusions are apparently inconsistent with the well-known results of Howard and Harvey (1970).

II. MEASUREMENT OF SOLAR ROTATION

The SSO instrument design is very similar to the solar magnetograph at the Mount Wilson 150 foot tower telescope (Howard, Tanenbaum, and Wilcox 1968; Howard and Harvey 1970; and Howard 1976*a*) but was designed for only low spatial resolution observations. Since some of the differences may affect rotation measurements, the relevant details will be described. The overall design philosophy of the SSO has been described by Scherrer *et al.* (1977). Preliminary rotation results and the modification to the instrument to allow full-disk 3′ magnetograms and Dopplergrams are described by Duvall (1979). Svalgaard, Scherrer, and Wilcox (1979) made a preliminary report of the conclusions to be described more fully in this paper. The results presented here differ slightly from the two earlier reports due to recalibration of the position, intensity, and velocity data. The calibration methods used in the present work are described below.

a) Position Calibration

The SSO telescope is outlined in Figure 1. The instrument consists of a vertical telescope with focal length of 6.5 m feeding a vertical 22.8 m Littrow spectrograph. The spectrograph is used in the 5th order with a reciprocal dispersion of 12.9 mm $Å^{-1}$ at 5250 Å. The entrance aperture consists of a 6 mm square mask, an image slicer, and a 0.75 mm × 100 mm slit. There are several systematic effects that must be examined when using this entrance aperture arrangement for low-resolution observations. These influence the effective position of the aperture on the Sun and the measured velocity.

The scanning system used is similar to most magnetograph instruments. A limb guider controls the orientation of the second-flat mirror with an analog servo system. The guider image is produced by an auxiliary lens with focal length of 7.0 m. The Sun is scanned by moving the guider north-south and east-west in steps of 0.001 inch. The position angle of the solar pole relative to the scanning axes is computed from the date and location of the coelostat mirror. The magnetogram/Dopplergram scan is made by stepping the image to fixed positions and integrating for 15 s at each location, instead of with a continuous motion. The scan is made in east-west lines (on the Sun) stepping 90″ between integrations with 180″ between lines. The aperture is 180″ square and is oriented parallel to the entrance slit which is north-south in the room. Prior to 1978 February 15 the aperture was rotated to be parallel to central meridian on the image, resulting in non-uniform illumination of some of the image slicer segments. Although no difference in the velocity data

[1]Now at Universite de Liège, Institut d'Astrophysique, Cointe-Ougrée, Belgium.

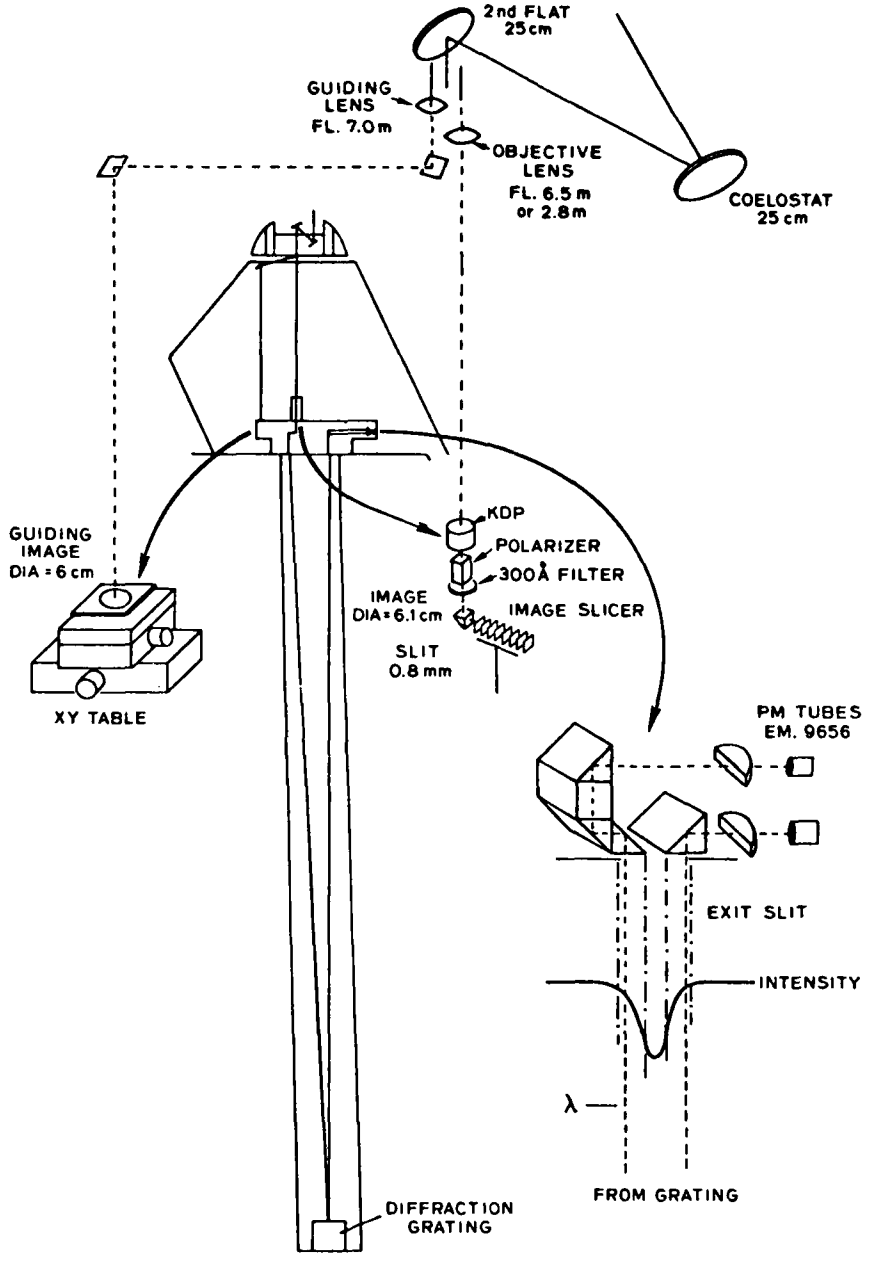

FIG. 1.—A schematic diagram of the Stanford Solar Telescope. Note the separate light path for the guider image and the observing image. The actual distance between the guider lens and the guider photodiodes is used to define the telescope scale. The spectrograph head is at ground level with the Littrow lens and diffraction grating at the bottom of a 23 m pit.

was found for several pairs of observations with the aperture oriented each way, there is less risk of systematic errors with the present alignment.

In order to measure solar rotation the conversion between scanner coordinates and effective heliocentric coordinates must be accurate. The telescope scale is defined by the 6.97 m distance between the guiding lens and the scanning table. The angular size of the solar disk is computed for the day of observation, and the geometrical position on the disk is found for each scanner position. If the observing aperture were only a few arcsec wide this would be sufficient to define the

heliocentric position; however, with a 180″ aperture the limb darkening across the aperture will weight the effective position of the aperture toward the center of the disk. An effective position is computed for each actual aperture position using the average observed limb-darkening function. For the aperture position at the limb, the correction is about a third the aperture size. The correction decreases rapidly away from the limb. For the rotation analysis described below, only the center half of the area of the disk is used, i.e., only points within 0.75 of a radius of the center of the disk. The maximum position correction for the points used is 4″. If the correction were omitted from the rotation analysis the computed equatorial rotation rate would be 0.25% too low (about 5 m s^{-1}).

b) Intensity Calibration

As part of normal magnetograph operation the brightness of the image is recorded during each integration. This is primarily used to compensate the magnetic field signal for brightness fluctuations. For each scan the individual intensity measurements are corrected for limb darkening and averaged over the center half of the disk. The variance of this quantity is used as a part of a quality figure for the scan. The magnitude of the average intensity will depend on the zenith angle, the photomultiplier tube voltage, the sky quality, and the cleanliness of the optics. Since the phototube voltages are rarely changed (twice per year) this quantity can be used to monitor the cleanliness of the sky and optics. When it was discovered that the average intensity could also be used to compute a correction for the effect of scattered light on the velocity observations, an effort was made to calibrate the intensity for the phototube voltages used since the start of the observations.

When the telescope is not making a magnetogram or some special observation, it is used for mean solar magnetic field observations. There are therefore several measures of the intensity of integrated sunlight for each day. All of the intensity observations for each day were plotted on a log scale as a function of computed air mass. A typical plot is shown in Figure 2. It can be seen that the expected linear relationship is found. The intercept corresponds to the intensity that would have been observed without the intervening atmosphere.

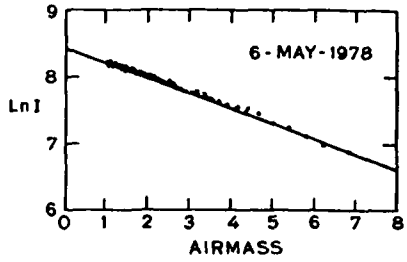

FIG. 2.—The change in observed image brightness as a function of air mass on a typical day. The intercept for zero air mass provides the calibration of the instrument intensity signal for that day.

From a plot of the intercept value as a function of date, the intensity changes resulting from phototube voltage changes were found. The calibrated disk average intensity from the magnetograms is plotted in Figure 3. Most of the variation with time is due to the varying amount of dirt on the optics. The arrows show the times that the coelostat mirror and lenses were cleaned.

c) Velocity Calibration and Corrections

The velocity observations are made by measuring the position of the spectral line. The spectrograph exit aperture consists of a pair of prisms mounted such that each prism gets light from one wing of the line and directs it to a photomultiplier tube. The prism assembly is mounted on accurate ways and positioned by a precise measuring screw. A shaft encoder is used to record the position of the prisms while a servo system keeps them centered on the line. One count of the encoder corresponds to 1/4096 of a turn of the screw with 10 turns per inch. Thus, for the dispersion at 5250 Å, the velocity calibration is 2.752 m s^{-1} per encoder count. This corresponds to about 0.6 μm of physical displacement of the prisms and is about the practical limit for a mechanical measuring engine. The rms variation due to spectrograph seeing, electronic noise, and servo errors is typically 10 m s^{-1} for a 15 s observation in integrated light. The velocity calibration is measured each day as part of a series of automatic checks; however, since the uncertainty in the daily measurement of dispersion is larger than the variations, a constant value is used for the data reported here.

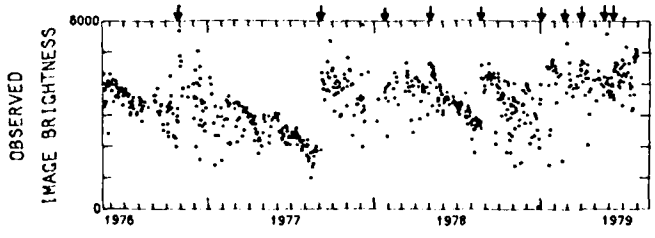

FIG. 3.—Observed image brightness for each magnetogram through 1979 July. The arrows show the dates on which the optics were cleaned. Intensity changes due to other instrument changes have been removed.

Before the observed line position data can be interpreted as motions of the Sun, the relative motion of the observatory and the Sun must be removed and spectrograph drifts must be removed. The Doppler shifts resulting from the Earth's rotation and orbital motion are removed for each point observed using the method described by Howard and Harvey (1970) and Howard, Boyden, and LaBonte (1980).

Other sources of drift in the velocity data include a slow motion of the diffraction grating during the first hour after it is repositioned, changes in the index of refraction of the air in the spectrograph, and drifts in the relative gain of the phototubes. To reduce the effect of the grating drift, the start of each scan is delayed for about a half-hour after the grating is positioned. In order to remove the remaining drifts from the data, a pair of 5 minute integrations is made at the center of the disk, one before and one after the scan. It is assumed that the drifts are linear in time, and these two disk-center averages are used to define the zero line. Figure 4 shows the total amount of this drift for each of the observations used for this study.

Once the relative motions and drifts are removed, the rotation rate of the photosphere can be computed. The first question one must address when measuring solar rotation is how to describe that rotation. The traditional method has been to assume that the antisymmetrical part of the Dopplergram can be described by a relation of the form:

$$\omega = a + b\sin^2 B + c\sin^4 B + \text{other terms}, \qquad (1)$$

where ω is the angular velocity, B is the heliographic latitude, and a, b, and c are to be found from a least-squares or other fit to the data (e.g., Howard and Harvey 1970). We use the same general method with a few differences. Since the observed quantity is a line-of-sight velocity and some of the systematic errors are shifts in apparent wavelength, we choose to express the determined coefficients and thus the rotation rate in m s^{-1} rather that rad s^{-1}. This necessitates conversion of the final result to angular velocity for comparisons but is more convenient for studying the various systematic effects. The limb redshift is assumed to be symmetrical about central meridian so that it will not affect the rotation-rate terms and is not explicitly removed. The magnitude of the limb shift is expected to be about 30 m s^{-1} at the boundary of the 0.75 $R_\odot$ disk used for the rotation studies and will be discussed in a future paper. Since an error in the computed position angle of the solar pole will produce an apparent north-south velocity at the expense of rotation, the linear antisymmetrical part of the velocity in the north-south direction is also found.

The form for differential rotation used is the same as used by Howard and Harvey (1970), but we make the assumption that the terms b and c in (1) have the same value. There is a computational problem resulting from the nonorthogonality of the terms used to describe rotation (Duvall and Svalgaard 1978; Stenflo 1977). The effect of this is that noise in the data will shift the amplitude between the b and c terms. Since the time-averaged values of b and c are about the same when (1) is used to determine rotation, it is assumed here that $b=c$. Any errors resulting from this assumption will appear as stable features in the residuals and will be examined in a later paper. In any case, the assumed equality of b and c has a negligible effect on the a coefficient.

Since the observed quantity is the line-of-sight component of velocity, and since rotation results in a purely azimuthal motion, the correction factor $\cos B \cos B_0 \sin L$ is used, where B_0 is the heliographic latitude of the disk center and L is the heliographic longitude measured from disk center. Thus the relation used to express rotation has the form:

$$V = \left[e + b\sin^2 B(1+\sin^2 B) \right] \times \cos B \cos B_0 \sin L + p \sin B. \qquad (2)$$

The coefficients e, b, and p in (2) are found for each scan by the method of least squares with each of the data values weighted by the intensity corrected for limb darkening. This weighting helps ensure that an occasional cloud will not adversely affect the results. Once

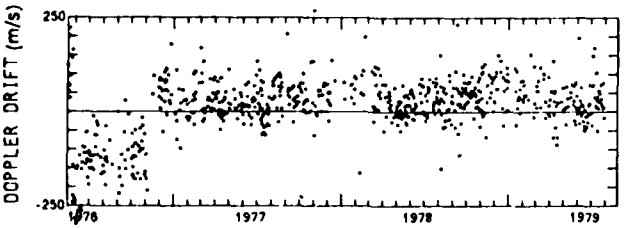

FIG. 4.—Drift in the velocity signal ascribed to spectrograph and electronics drifts. The total amount of the drift between the reference integrations is shown. The average magnitude of the drift was 43 m s^{-1} hr^{-1}. The algorithm for positioning the grating was changed in 1976 October to reduce the residual grating motion.

the coefficients above have been found, the error in the position angle can be found from

$$p_{\rm err} = \tan^{-1}(p/e),$$

and the equatorial rotation velocity is found from

$$a = \sqrt{e^2 + p^2}\ .$$

In practice, $p_{\rm err}$ has been found to be small with a typical value of 0°.1. In addition to the terms a, b, and $p_{\rm err}$ found above, a term a_0 is found from a second fit to the data with the term b replaced with a constant -300 m s^{-1}. The coefficients a_0, a, and b have been found for all reasonable completed scans to date. Of the total 975 scans 244 were eliminated because they were incomplete or were made during such bad weather the data were obviously not useful.

In addition to the above corrections, there are two types of systematic effect that should be considered for the SSO instrument. These are the alignment of the entrance slit and the exit slit and the presence of significant amounts of scattered light for the earlier observations. (We now keep the optics scrupulously clean so that scattered light is of the order of one part in a thousand.)

The combined effect of the use of an image slicer, a 3′ aperture, and the north-south direction of the entrance slit results in a signal in the same sense as solar rotation if the exit slit is not exactly parallel to the entrance slit. Prior to 1978 February 15 there was a small misalignment that caused such an error (as described by Duvall 1979). In addition to altering the observed rotation rate, the misalignment of the slits results in an apparent change in rotation with distance from disk center. The net effect can be clearly seen by comparing uncorrected Dopplergrams for observations before and after the slit readjustment. Figure 5 shows two such Dopplergrams. The closed contours at the east and west limbs in Figure 5*a* are the result of the misalignment. An analysis of the correlation between the equatorial rotation rate and intensity (as described below) shows that the data before the slits were properly adjusted should be increased by 2.1%. This correction has been included in the results presented here.

III. EFFECT OF SCATTERED LIGHT

a) The Problem

Figure 6 shows the observed equatorial rate a_0 corrected for all the effects described above. The general character of the data is a sequence of slow declines followed by sudden increases. The arrows show the times that the coelostat mirror was removed and cleaned or resurfaced. There is a clear connection between the times of cleaning and the times of sharp increase in observed rotation rate. The correlation between the observed brightness shown in Figures 3 and 6 is also obvious. After each cleaning of the optics, the intensity and a_0 both jump. As dust and smog accumulate on the mirrors and lens, both the intensity of the image and the observed rotation rate decrease. This correlation is to be expected since as the dust scatters light out of the main beam, it mixes light from the entire disk with light from a particular region.

The details of the expected effect depend on the density of scattering sources, the size and height distribution of the particles, and the angular aperture of the instrument. In any case it is expected that the effect on the rotation rate will be proportional to the scattered brightness just off the limb. Because of the limited angular aperture the effective intensity of the scattered light will be proportional to the density of scatterers while the direct intensity will decrease exponentially with the number of scatterers. Therefore, in the analysis below, the natural logarithm of the intensity is used for comparison to the rotation rate. The

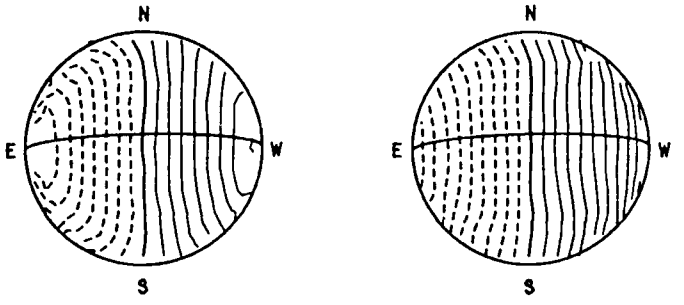

FIG. 5.—Solar velocity contours as observed. Dashed contours are motion toward the observer, solid away. The contour interval is 200 m s^{-1}. A solid-body rotation would result in straight vertical contours. Data for two days is shown: (*a*) (1978 February 15) observed with an entrance slit alignment error that affects velocity measurements near the limb; (*b*) (1978 March 16) typical for observations with the correct alignment.

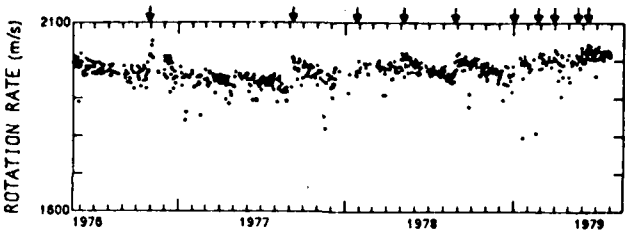

FIG. 6.—Solar equatorial rotation rate a_0 for each magnetogram scan included in this analysis. There are tick marks at the first of each month. The arrows show the dates of cleaning and realuminizing the mirrors.

effect of scattered light from the instrument and the sky on rotation measurements has been known for a long time (e.g., Plaskett 1915).

b) The Correction

Since there is an effect on the observed velocities due to scattered light, observation should only be made with clear skies and clean optics. In the past at the SSO this condition was not always met, but since the observations made in less than optimum conditions contain a significant amount of information about solar motions, we have attempted to remove as much of the effect of scattered light as possible. This is done by finding an empirical relation between the intensity I and a_0. We expect

$$I = I_0 e^{-T},$$

where T is the optical thickness. The scattered light intensity S off the limb (as a fraction of the disk center intensity) should be proportional to T, so we can write

$$I = I_0 e^{-kS}. \tag{3}$$

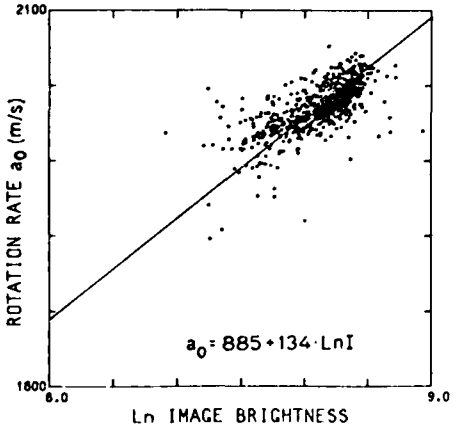

FIG. 7.—A scatterplot of the equatorial rotation rate a_0 as a function of the logarithm of the observed image brightness $\ln(I)$. The best-fit line shown is used to determine the error in a_0 which is due to the correlation with intensity.

The decrease in observed rotational velocity should be proportional to S, so we can write

$$V_{\text{obs}} = V_{\text{actual}} - \alpha S, \tag{4}$$

then combining (3) and (4) we expect

$$V_{\text{obs}} = V_{\text{actual}} - \alpha/k\,(\ln I_0 - \ln I). \tag{5}$$

Since V_{obs} and $\ln I$ are observed, α/k and $\ln I_0$ are needed to find V_{actual}. Figure 7 shows a scatterplot of V_{obs} and $\ln I$. The line is the least-squares linear regression line $V = 134 \ln I + 885$. A separate analysis for data before and after 1978 February 15 yielded the 2.1% correction to compensate for the slit adjustment described above.

To complete the correction we need to know I_0, that is, the intensity (corrected for phototube changes) that would have been found with clean sky and optics. Since 1978 August the scattered light intensity just off the limb has been measured at the start of each scan. Figure 8*a* shows $\ln I$ versus S. The intercept of the best-fit line yields $\ln I_0 = 8.56$. Thus we have

$$V_{\text{corrected}} = V_{\text{obs}} + 134(8.56 - \ln I). \tag{6}$$

Figure 8*b* shows the correlation between the observed rotation velocity and the measured scattered light. The roughly linear relationship here justifies the form of equation (4). The slope of the line in Figure 8*b* is the term α in equation (4), and similarly Figure 8*a* provides directly a value for k in equation (3). These combine to yield $\alpha/k = 119$ which is in close agreement with the value for α/k derived from the direct comparison of intensity and rotation in Figure 7. Owing to uncertainties in assessing the relative errors in the computed rotation rate and the observed scattered light, the slopes of the lines in Figures 8*a* and 8*b* have poorly determined errors. The expected maximum value for the slope in Figure 8*b* is about 20 m s^{-1} per percent scattered light. Inspection of Figure 8 shows that a smaller value of the slopes of the lines is consistent with the data, with the expected value of 20 m s^{-1} per percent scattered light, and with the ratio α/k found in Figure 7.

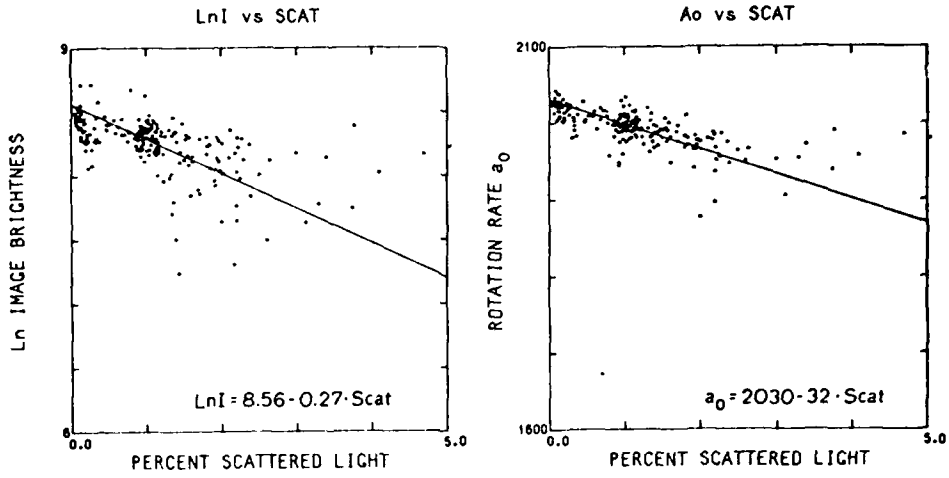

FIG. 8.—Scatterplots of (*a*) ln(*I*) and (*b*) a_0 with the observed scattered light *S* for those observations for which *S* was measured. The quantity *S* is the brightness in the 3′ aperture centered about 2′ off the limb relative to the disk center brightness. The intercept in Fig. 8*a* shows the brightness with no scattered light I_0, while the slope of the best-fit lines in Figs. 8*a* and 8*b* verify the correction factor derived in Fig. 7.

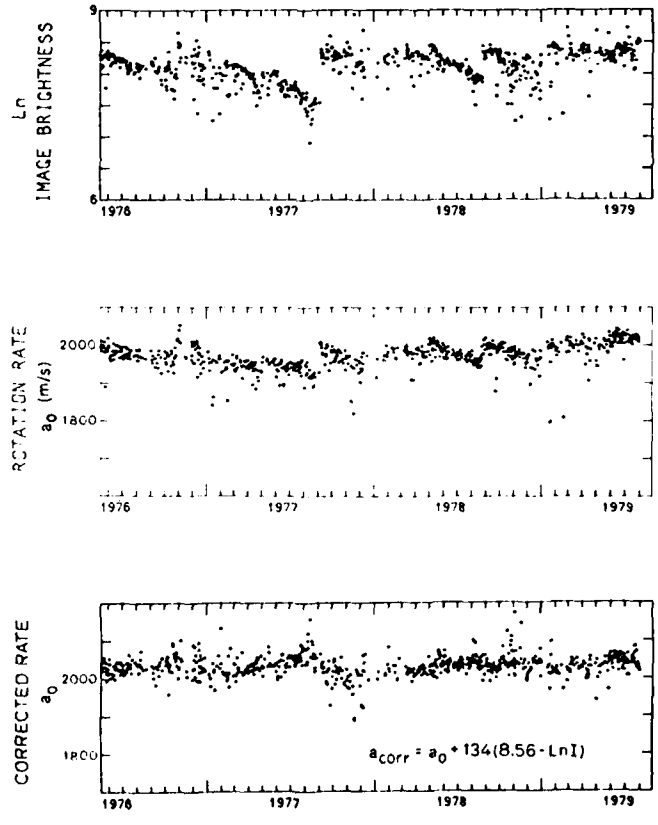

FIG. 9.—(*a*) The observed image brightness (from Fig. 3); (*b*) the observed rotation rate a_0 (from Fig. 6); and (*c*) the corrected equatorial rotation rate for all included scans. The correction was applied separately for each scan; thus some of the variance in brightness which is not correlated with scattered light tends to increase the variance in the corrected rotation rate. The estimate for day-to-day variations in a_0 is made from Fig. 9*b* disregarding the drift resulting from the correlation with 9*a*.

IV. DISCUSSION

a) The Variability of Solar Rotation

Figure 9c shows the equatorial rotation rate a_0 as corrected with relation (6). Figure 9a is the logarithm of the brightness data from Figure 3, and Figure 9b is the data from Figure 6 shown here for comparison. Several statements concerning the nature of solar rotation can be made by examining these data. The first and most certain is that the day-to-day variation in the observed value is small with an rms variation from the mean of 26 m s^{-1} or about 1.3%. During intervals of good weather, as indicated by small variance in the intensity, it can be seen that the solar contribution to the observed velocity variations is probably smaller than 20 m s^{-1}. These relatively small upper limits for the short-term fluctuations in solar rotation are noticeably smaller than the values previously reported for Doppler-shift-type observations.

Examination of Figure 9 also shows that there are no identifiable seasonal or yearly variations during the 3 years of available data that exceed 20 m s^{-1}. This can be confirmed from Figure 10 which is the result of a 108 day low-pass filtering of Figure 9c. Considering the uncertainties in the corrections applied, there is no justification for concluding that even these small variations are of solar origin. There may, of course, be long-term variations in the rotation rate that are masked by uncertainties in the corrections. While variations larger than 1% seem to be excluded by this analysis, a 1% increase in 3 years (as suggested by Howard 1976b and by Livingston and Duvall 1979) could have been masked by an error in the slit alignment correction.

b) Actual Value of Solar Rotation

Newton and Nunn (1951) reported the average rotation rate of long-lived recurrent sunspots. Using their form for differential rotation, the equatorial rate from sunspot observations is 2020 m s^{-1}. An inspection of Figure 9 shows that, to the certainty of the corrections, the photospheric material also rotates at this rate. Considering the possible uncertainty in the corrections it is worthwhile to examine separately the data since 1979 May 18. While this represents only 60 observations, the scattered light has been low enough that no correction is necessary. Figure 11 shows this data. There has been no change in the procedure during this time except to keep the optics clean to exclude an effect from scattered light. The average value of the uncorrected rate a_0 for this interval is 2016 ± 13 m s^{-1}. In order to be fully confident of the constancy of this value, an additional year or more of observations must be made, but it is safe to say that in 1979 June the photospheric material rotated at the Newton and Nunn rate.

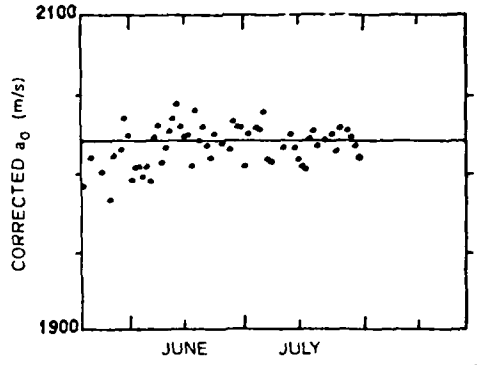

FIG. 11.—The observed (uncorrected) equatorial rate for the most recent data (clean optics). The horizontal line is drawn at the Newton and Nunn rate of 2020 m s^{-1}. The simple mean of the data shown is 2016 m s^{-1} with a standard deviation of 13 m s^{-1}.

V. CONCLUSIONS

Several points need to be reviewed. At the SSO, measurements of the solar rotation rate have been made since 1976 May. In the earlier observations, the measured velocities were contaminated by scattered light. This is exhibited by an obvious correlation between the observed intensity and velocity data. When the effect of scattered light is removed by empirical methods it is found that (a) the day-to-day variations in the equatorial rotation are at most 20 m s^{-1} rms about the mean; (b) there are no long-term trends exceeding 1% that can be associated with the Sun rather than the instrument; and (c) the average rate

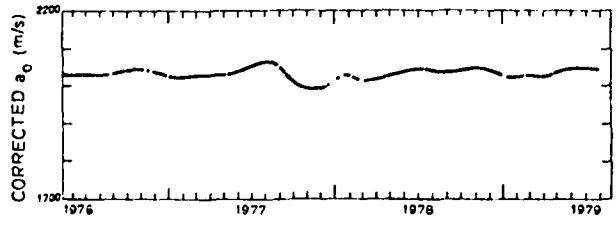

FIG. 10.—Slow drifts in the corrected equatorial rate. A 108 day low pass filter has been applied. The trends in this figure are probably due to the incomplete removal of instrumental problems.

for the photosphere is most likely about the same as the Newton and Nunn rate for sunspots. Point (*b*) is not yet in conflict with the results of Howard (1976*b*) and Livingston and Duvall (1979).

It was also found that the fewer the number of terms used to express solar rotation the smaller the variance in the rate determined. When the term for differential rotation is also fitted to the data the rotation is found to be:

$$V = 2030 - 278 \sin^2 B - 278 \sin^4 B \text{ m s}^{-1}$$

(at one solar radius), which is the same as

$$\omega = 2.917 - 0.40 \sin^2 B - 0.40 \sin^4 B \ \mu\text{rad s}^{-1}.$$

These conclusions are different from the commonly held belief that the photosphere in general rotates slower than large-scale magnetic field structures and that the rate shows substantial variations. It is unlikely that magnetograph-type observations made at other observatories suffer from the specific errors that formerly existed at the SSO (e.g., scattered light), but there may be some as yet unidentified sources of instrumental noise. If there is some noise which is not purely random then the observations may not be in conflict, but only the interpretations.

This work was assisted by discussions at the Workshop on Solar Rotation Observations held at Hale Observatories in 1979 March. This work was supported in part by the Office of Naval Research under Contract N00014-76-C-0207, by the National Aeronautics and Space Administration under grant NGR 05-020-559 and contract NAS5-24420, and by the Division of Atmospheric Sciences, Solar Terrestrial Research Program of the National Science Foundation under grant ATM77-20580.

REFERENCES

DeLury, R. E. 1939, *J.R.A.S. Canada*, **33**, 345.
Duvall, T. L., Jr. 1979, *Solar Phys.*, **63**, 3.
Duvall, T. L., Jr., and Svalgaard, L. 1978, *Solar Phys.*, **56**, 463.
Hart, A. B. 1954, *M.N.R.A.S.*, **114**, 2.
Howard, R. 1976*a*, *Solar Phys.*, **48**, 411.
———. 1976*b*, *Ap. J. (Letters)*, **210**, L159.
———. 1978, *Rev. Geophys. Space Phys.*, **16**, 721.
Howard, R., Boyden, J. E., and LaBonte, B. J. 1980, *Solar Phys.*, in press.
Howard, R., and Harvey, J. 1970, *Solar Phys.*, **12**, 23.
Howard, R., Tanenbaum, A. S., and Wilcox, J. M. 1968, *Solar Phys.*, **4**, 286.
Livingston, W., and Duvall, T. L., Jr. 1979, *Solar Phys.*, **61**, 219.
Newton, H. W., and Nunn, M. L. 1951, *M.N.R.A.S.*, **111**, 413.
Plaskett, H. H. 1973, *M.N.R.A.S.*, **163**, 183.
Plaskett, J. S. 1915, *Ap. J.*, **42**, 373.
Scherrer, P. H., Wilcox, J. M., Svalgaard, L., Duvall, T. L., Jr., Dittmer, P. H., and Gustafson, E. K. 1977, *Solar Phys.*, **54**, 353.
Stenflo, J. O. 1977, *Astr. Ap.*, **61**, 797.
Svalgaard, L., Scherrer, P. H., and Wilcox, J. M. 1979, *Proc. Workshop on Solar Rotation*, ed. G. Belvedere and L. Paterno, Osservatorio Astrofisico di Catania, Publicazione No. 162, 151.

P. H. SCHERRER and J. M. WILCOX: Institute for Plasma Research, Stanford University, Via Crespi, Stanford, CA 94305

L. SVALGAARD: Université de Liège, Institut d'Astrophysique, Cointe-Ougrée, Belgium

Reprint Series
1 August 1980, Vol. 209, pp. 603-605

SCIENCE

Origin of the Warped Heliospheric Current Sheet

J. M. Wilcox, J. T. Hoeksema, and P. H. Scherrer

Origin of the Warped Heliospheric Current Sheet

Abstract. *The warped heliospheric current sheet for early 1976 is calculated from the observed photospheric magnetic field by a potential field method. Comparisons with measurements of the interplanetary magnetic field polarity for early 1976 obtained at several locations in the heliosphere by Helios 1, Helios 2, Pioneer 11, and at the earth show a rather detailed agreement between the computed current sheet and the observations. It appears that the large-scale structure of the warped heliospheric current sheet is determined by the structure of the photospheric magnetic field and that "ballerina skirt" effects may add small-scale ripples.*

The magnetic field of the sun is extended outward by the solar wind throughout the solar system. The structure of the extended field has been observed only within 16° of latitude of the solar equator, so that its overall form, containing the well-known magnetic sectors near the equatorial plane, has been a matter of conjecture and debate for many years. The Solar Polar Mission, sometime in the next decade, will probably settle the major questions by direct observation in space. This report describes our present view of the extended structure of the solar magnetic field.

The existence of a warped current sheet in the nonpolar regions of the heliosphere is now generally accepted (*1–4*). An artist's impression of an average shape of the current sheet at a time near sunspot minimum (*2*) is shown in Fig. 1. As the current sheet rotates with the sun, the sector structure of the interplanetary magnetic field (IMF) is produced (*5*). At the phase of the sunspot cycle discussed in this report, the large-scale IMF is directed away from the sun northward of the current sheet and is directed toward the sun southward of the sheet. It should be noted that the term "interplanetary sector structure" coined by Wilcox and Ness (*5*) describes the structure in the plane of the ecliptic and does not refer to three-dimensional structures such as the sections of an orange.

There are two points of view regarding the origin of the warped heliospheric current sheet. Svalgaard and Wilcox (*6*) review the computations of the magnetic field at a "source surface," for which the photospheric magnetic field observed by use of the Zeeman effect serves as a boundary condition. Outside the source surface the warped current sheet is assumed to be carried radially outward by the solar wind. In this model, the structure of the current sheet (the location in solar longitude and the extent in solar latitude of the maxima and minima) is a direct consequence of the observed photospheric magnetic field.

Alfven (*4*) [see also (*7*)] has proposed an alternative viewpoint in which the solar origin of the current sheet is a plane similar to the plane in which the skirt of a ballerina originates (the waist). In this model the current sheet waves up and down like the skirt of a spinning ballerina.

It is our purpose in this report to show that the observations of the IMF during the first months of 1976 (that is, near sunspot minimum) at the earth—by Pioneer 11 near a heliospheric latitude of 16°N (*8*) and by Helios 1 and Helios 2 between 0.28 and 1 A.U. within a latitudinal excursion of ±7.23° from the solar equatorial plane (*9*)—are in good agreement with a warped current sheet computed from the observed photospheric magnetic field by the methods reviewed in (*6*). It thus appears that the large-scale structure of the heliospheric current sheet is controlled by the photospheric magnetic field, although small-scale ripples may be added by dynamic solar wind processes (the ballerina effect).

The curved line in Fig. 2 represents the average warped current sheet that separates regions with magnetic field away from the sun (above the line) and toward the sun (below the line), as computed on a source surface at 2.6 solar radii during the interval 20 January through 26 May 1976. The solar wind is assumed to carry the magnetic structure on the source surface radially outward into the heliosphere. In fact, the curved line in Fig. 2 is similar to the bottom panel of figure 4 in (*6*), which was computed as the average of eighteen 27-day solar rotations starting 5 May 1976 and ending 7 August 1977, just after the interval discussed in this report. This similarity is evidence of the long-term stability of the large-scale photospheric and heliospheric magnetic fields.

Such long-term stability would not be expected from the dynamic effects of the ballerina skirt model. Nor would this stability be expected if the predominant warps in the current sheet were caused by coronal holes (*9*), since the lifetime of a coronal hole is typically only several rotations. Because coronal holes appear in the central portion of sectors (*6*), it would be expected that the longitudes of coronal holes would correspond to the

Fig. 1. Artist's impression of the warped heliospheric current sheet. The region above the current sheet has interplanetary magnetic field directed away from the sun and the region below has field directed toward the sun. [Artist: Werner Heil]

0036-8075/80/0801-0603$00.50/0

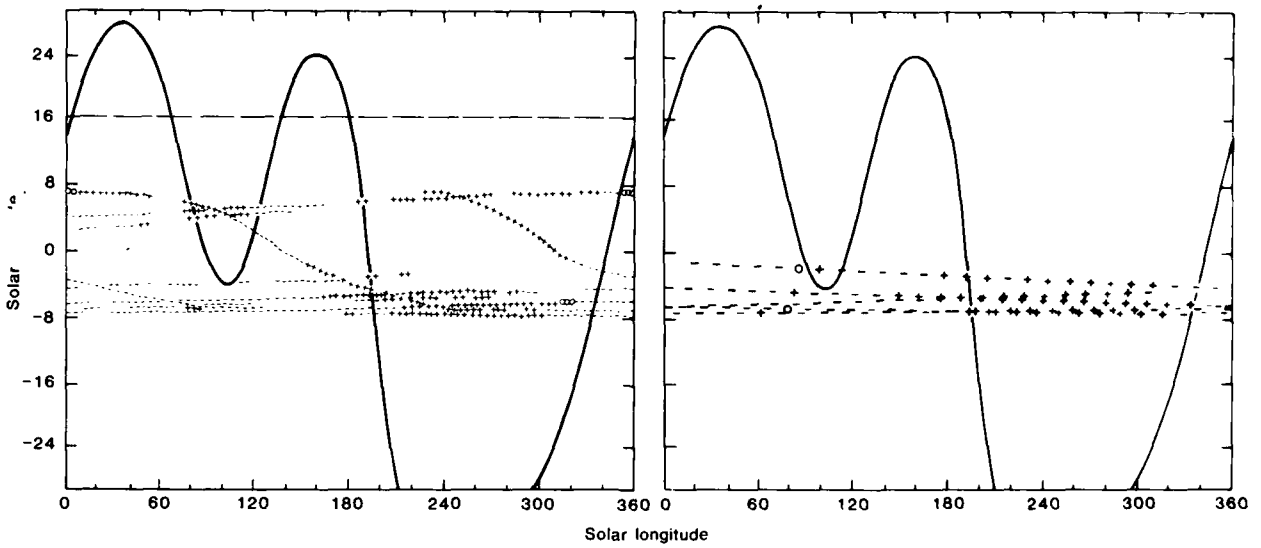

Fig. 2. The curved line represents the calculated average heliospheric current sheet for five rotations from 20 January through 23 May 1976. The dashed line at 16°N latitude represents the approximate heliographic latitude of the Pioneer 11 spacecraft, which was about 4 A.U. from the sun. The plus signs (away from the sun) and minus signs (toward the sun) indicate the IMF polarity measured at Helios 1 and Helios 2 projected back onto the solar corona. The observed IMF polarities agree well with the computed current sheet. Fig. 3. Same as Fig. 2, except that the plus and minus signs represent the inferred IMF polarity at the earth mapped back to the solar corona. The observed polarity changes occur near crossings of the computed current sheet.

longitudes of maximum warp of the heliospheric current sheet.

The dashed horizontal line in Fig. 2 represents the heliographic latitude 16°N, near which Pioneer 11 observed the IMF to be predominantly away from the sun during the interval discussed in this report (*8*). The plus (away) and minus (toward) signs in Fig. 2 represent the IMF polarity as observed by Helios 1 and Helios 2 (*9*) projected onto the solar corona. The computed current sheet in Fig. 2 is similar to the inferred current sheet shown in figure 4b of (*9*).

Figure 2 shows that the Helios spacecraft observations of the polarity of the IMF are in good agreement with the computed location of the current sheet. When the Helios spacecraft were at southern heliographic latitudes a two-sector pattern was observed, whereas when they were at northern latitudes a four-sector pattern was observed, in agreement with Fig. 2.

The curved line in Fig. 2 representing the warped heliospheric current sheet is repeated in Fig. 3, where the plus and minus signs show the inferred IMF polarity at the earth (*10*). A travel time of 4.5 days from the sun to the earth (*11*) is used in mapping this back to the corona. The IMF structure at the earth also shows a two-sector pattern when the earth is near 7°S heliographic latitude, but hints of the four-sector structure are seen as the earth moves northward.

We note that if a travel time of 5.5 days had been used, the data in Fig. 3 would be moved to the right by about 13° of longitude, which would significantly improve the agreement. The same situation exists with regard to the spacecraft data in Fig. 2. This suggests that the simple mapping techniques used in preparing Figs. 2 and 3 may give only an approximation.

Although the large-scale structure of the current sheet persists for many solar rotations, on any particular rotation there may be changes in the current sheet arising from the effects of solar activity and coronal holes (*12*). Nevertheless, the overall agreement in Figs. 2 and 3 between the observed IMF polarities and the structure of the heliospheric current sheet computed from the observed photospheric magnetic field is impressive.

From the considerations discussed in this report we suggest that if Pioneer 11 had been at 16°S heliospheric latitude in the first part of 1976 rather than at 16°N, it would have observed a well-defined sector structure. Also, although Pioneer 11 did observe an IMF polarity that was predominantly away from the sun, we would predict that for intervals of a few days corresponding to Carrington solar longitudes near 35° and 160°, Pioneer 11 may have observed "toward" polarities. We note in figure 2 of Smith *et al.* (*8*) that during the interval of interest the ratio of the number of "away" polarity observations by Pioneer 11 to the total number of observations was about 0.8. The computed current sheet in Fig. 2 of this report corresponds to a ratio of about 0.7.

We suggest that the observations of the IMF polarity by Pioneer 11 and by Helios 1 and Helios 2 support the view that the large-scale structure of the warped heliospheric current sheet can be computed from the observed photospheric magnetic field, with the ballerina effect perhaps adding small-scale ripples. Since coronal holes are effects of conditions pertaining to the large-scale photospheric magnetic configuration (*6*), the influence of coronal holes on the warped current sheet is to a considerable extent already included in the present calculations.

The observations by Pioneer 11 at 16°N heliospheric latitude (*8*) have been misinterpreted as meaning that the heliospheric current sheet is almost parallel to the solar equatorial plane [for example, see (*13*)]. Figure 2 shows that even near the minimum of the 11-year sunspot cycle the current sheet probably reached appreciable south heliospheric latitudes, and the considerations discussed by Svalgaard and Wilcox (*2*) indicate that near the maximum of the sunspot cycle the current sheet reaches heliospheric latitudes of 50° or more (*3*).

J. M. WILCOX
J. T. HOEKSEMA
P. H. SCHERRER
Institute for Plasma Research, Stanford University, Via Crespi, Stanford, California 94305

References and Notes

1. K. H. Schatten, in *Solar Wind*, C. P. Sonett, P. J. Coleman, Jr., J. M. Wilcox, Eds. (National Aeronautics and Space Administration, Washington, D.C., 1972), p. 88; M. Schulz, *Astrophys. Space Sci.* **24**, 371 (1973); E. H. Levy, *Nature (London)* **261**, 394 (1976); M. Schulz, E. N. Frazier, D. F. Boucher, Jr., *Sol. Phys.* **60**, 83 (1978).
2. L. Svalgaard and J. M. Wilcox, *Nature (London)* **262**, 766 (1976).
3. T. Saito, *Sci. Rep. Tohoku Imp. Univ. Ser. 5* **23**, 37 (1975).
4. H. Alfven, *Rev. Geophys. Space Phys.* **15**, 271 (1977).
5. J. M. Wilcox and N. F. Ness, *J. Geophys. Res.* **70**, 5793 (1965).
6. L. Svalgaard and J. M. Wilcox, *Annu. Rev. Astron. Astrophys.* **16**, 429 (1978).
7. E. J. Smith and J. H. Wolfe, *Space Sci. Rev.* **23**, 217 (1979).
8. E. J. Smith, B. T. Tsurutani, R. Rosenberg, *J. Geophys. Res.* **83**, 717 (1978).
9. U. Villante, R. Bruno, F. Marini, L. F. Burlaga, N. F. Ness, *ibid.* **84**, 6641 (1979).
10. L. Svalgaard, *ibid.* **77**, 4027 (1972).
11. J. M. Wilcox, *Space Sci. Rev.* **8**, 258 (1968).
12. R. H. Levine, *Astrophys. J.* **218**, 291 (1977); in *Coronal Holes and High Speed Wind Streams*, J. Zirker, Ed. (Colorado Associated Univ. Press, Boulder, 1977), pp. 103–143.
13. M. A. Livshits, T. E. Valchuk, Y. I. Feldstein, *Nature (London)* **278**, 241 (1979).

14. We thank R. Howard for observations of the photospheric magnetic field obtained at Mount Wilson Observatory. This work was supported in part by the ONR contract N00014-76-C-0207, by NASA grant NGR 05-020-559 and contract NAS5-24420, and by the Atmospheric Sciences Section of the National Science Foundation under grant ATM77-20580.

18 March 1980; revised 5 May 1980